

# 1 Quantifying legacies of clearcut harvesting on carbon fluxes 2 and biomass carbon stock in northern temperate forests

3 W. Wang<sup>1\*</sup>, J. Xiao<sup>1</sup>, S. V. Ollinger<sup>1</sup>, A. R. Desai<sup>2</sup>, J. Chen<sup>3</sup>, A. Noormets<sup>4</sup>

4 [1] {Earth Systems Research Center, Institute for the Study of Earth, Oceans, and Space,  
5 University of New Hampshire, Durham, NH 03824, USA}

6 [2] {Department of Atmospheric & Oceanic Sciences, University of Wisconsin-Madison,  
7 Madison, WI 53706, USA}

8 [3] {Center for Global Change & Earth Observations, Department of Geography, Michigan State  
9 University, East Lansing, MI 48823, USA}

10 [4] {Department of Forestry and Environmental Resources, North Carolina State University,  
11 Raleigh, NC 27695, USA}

12 [\*]Now at: Department of Geography, McGill University, Montreal, QC H3A 0B9, Canada}

13 Corresponding to W. Wang ([wang.weifeng@unh.edu](mailto:wang.weifeng@unh.edu))

## 14 15 **Abstract**

16 Stand-replacing disturbances including harvests have substantial impacts on forest carbon  
17 (C) fluxes and stocks. The quantification of these effects is essential for better understanding of  
18 forest C dynamics and informing forest management in the context of global change. We  
19 evaluated a process-based forest ecosystem model, PnET-CN, for how and by what mechanisms  
20 clearcuts alter ecosystem C fluxes, aboveground C stocks (AGC), and leaf area index (LAI). We  
21 compared the effects of stand-replacing harvesting on C fluxes and stocks using two  
22 chronosequences of eddy covariance flux sites for deciduous broadleaf forests (DBF) and  
23 evergreen needleleaf forests (ENF) in the Upper Midwest region of northern Wisconsin and  
24 Michigan, U.S.A. The average normalized root mean square error (NRMSE) and the Willmott  
25 index of agreement ( $d$ ) for carbon fluxes, LAI, and AGC in the two chronosequences were 20%  
26 and 0.90, respectively. Simulated gross primary productivity (GPP) increased with stand age,  
27 reaching a maximum ( $\sim 1200\text{--}1500\text{ g C m}^{-2}\text{ yr}^{-1}$ ) at 11–30 years of age, and leveled off thereafter  
28 ( $\sim 900\text{--}1000\text{ g C m}^{-2}\text{ yr}^{-1}$ ). Simulated ecosystem respiration (ER) for both plant function types

1 (PFTs) was initially as high as  $\sim 700\text{--}1000 \text{ g C m}^{-2} \text{ yr}^{-1}$  in the first or second year after harvesting,  
2 decreased with age ( $\sim 400\text{--}800 \text{ g C m}^{-2} \text{ yr}^{-1}$ ) before canopy closure at 10–25 years of age, and  
3 increased to  $\sim 800\text{--}900 \text{ g C m}^{-2} \text{ yr}^{-1}$  with stand development after canopy recovery. Simulated net  
4 ecosystem productivity (NEP) for both PFTs was initially negative with net C losses of  $\sim 400\text{--}$   
5  $700 \text{ g C m}^{-2} \text{ yr}^{-1}$  for 6–17 years after clearcuts, reached the peak values of  $\sim 400\text{--}600 \text{ g C m}^{-2} \text{ yr}^{-1}$   
6 at 14–29 years of age, and became stable and a weak C sink ( $\sim 100\text{--}200 \text{ g C m}^{-2} \text{ yr}^{-1}$ ) in mature  
7 forests (>60 years old). The decline of NEP with age was caused by the relative flattening of  
8 GPP and gradual increase of ER. ENF recovered slower from net C source to net sink and lost  
9 more C than DBF, suggesting that ENF is likely slower to recover to full C assimilation capacity  
10 after stand-replacing harvests arising from slower development of photosynthesis with stand age.  
11 Model results indicated that increased harvesting intensity would delay the recovery of NEP after  
12 clearcut, but it had little effect on C dynamics during late succession. Future modeling studies of  
13 disturbance effects will benefit from the incorporation of forest population dynamics (e.g.,  
14 regeneration and mortality), relationships between age-related model parameters and state  
15 variables (e.g., LAI), and silvicultural practices into the model.

16

## 17 **1 Introduction**

18 Disturbance has been widely recognized as a key factor influencing ecosystem structure  
19 and function at decadal to century scales (Magnani et al., 2007; Williams et al., 2012; Kasischke  
20 et al., 2013). Harvest is an important anthropogenic disturbance shaping North American forest  
21 landscapes. Approximately  $61,000 \text{ km}^2$  of forests were affected by harvests every year during the  
22 2000s (Masek et al., 2011). Harvests affect forest age structure and alter the forest carbon (C)  
23 balance (Magnani et al., 2007; Pan et al., 2011; Williams et al., 2012). Quantifying the legacies  
24 of harvest disturbances under the context of climate change is essential for predicting forest C  
25 dynamics, informing climate policy-making, and improving forest management. Here, we focus  
26 on assessment of an ecosystem model C cycle response from one type of harvest, the clear-cut.

27 Harvests transfer living biomass C to harvested wood C and litter C, resulting in  
28 successional changes in C fluxes and stocks. Leaf biomass increases rapidly in secondary  
29 succession and then typically stabilizes at a certain level that is determined by light, water,  
30 nutrient availability, and forest type (Sprugel, 1985). Gross primary productivity (GPP) thus  
31 increases gradually over time, reaches maximum in middle age, and in response to nutrient

1 limitations and aging responses slightly declines thereafter (Odum, 1969; Chapin et al., 2002;  
2 Tang et al., 2014). The successional change in plant respiration (autotrophic respiration) after  
3 stand-replacing harvesting is similar to that of GPP, although C use efficiency (the ratio of net  
4 primary productivity to GPP, NPP/GPP) could decline with forest age (DeLucia et al., 2007). As  
5 a result, living tree biomass C gradually increases following a typical logistic growth curve  
6 (Odum, 1969; Sprugel, 1985).

7 Heterotrophic respiration following stand-replacing harvesting could be stimulated at the  
8 beginning of stand development because the removal of trees alters the environmental conditions  
9 (e.g., soil temperature, moisture, and nutrients) and possibly leads to changes in litter quantity  
10 depending on harvest types (e.g., stem-only harvesting) (Chapin et al., 2002). Heterotrophic  
11 respiration is expected to gradually decrease thereafter because the regrowing forest reduces net  
12 radiation, water, and nutrient availability to the soil (Chapin et al., 2002) and the amount of  
13 decomposable soil organic matter from the prior forest and harvest residue (e.g., litter, coarse  
14 woody debris, and soil organic C) also gradually decreases. Over time, however, heterotrophic  
15 respiration could again be enhanced because of accumulation of woody debris and litter with  
16 stand development. This theorized successional trajectory in ecosystem respiration (ER; the sum  
17 of autotrophic and heterotrophic respiration) may also be strongly influenced by harvest types  
18 and forest composition. Unlike GPP or NPP, the trajectory of heterotrophic respiration (and  
19 consequently total ecosystem respiration) with age is not as well-understood (Amiro et al., 2010).  
20 Observational studies to date have shown that forest ecosystems generally become C sources  
21 (negative net ecosystem productivity, NEP) immediately following stand-replacing harvests,  
22 approach the maximum NEP as they mature, and then experience a gradual decline in NEP  
23 thereafter (e.g., Law et al., 2003; Gough et al., 2007; Goulden et al., 2011), following the  
24 trajectories hypothesized by Odum (1969) and Chapin et al. (2002).

25 The changes of C fluxes and stocks after harvesting have been examined in many forest  
26 ecosystems using ecological measurements (e.g., eddy covariance observations) from  
27 chronosequences using a space-for-time substitution approach (e.g., Law et al., 2003; Gough et  
28 al., 2007; Goulden et al., 2011). The trajectories and amplitude of C fluxes and stocks vary with  
29 forest ecosystem types (Amiro et al., 2010). For example, Noormets et al. (2007) reported that a  
30 young red pine (*Pinus resinosa*) stand at 8 years of age was a net C sink ( $313 \pm 14 \text{ g C m}^{-2} \text{ yr}^{-1}$ ),  
31 but a young hardwood site at age of 3 was a net C source ( $-128 \pm 17 \text{ g C m}^{-2} \text{ yr}^{-1}$ ) over the growing

1 season in northern Wisconsin, U.S.A. Young stands in northern Wisconsin may become net C  
2 sinks within 10-15 years after harvesting (Noormets et al., 2007). More rapid recovery after  
3 stand-replacing harvesting (< 6 years) was found for temperate forests in northern Michigan  
4 (Gough et al., 2007). These studies have produced a wealth of information on ecosystem C  
5 dynamics after stand-replacing disturbances, and this information can be translated to more  
6 process-based and quantitative understanding of disturbance effects on the C cycle using  
7 ecosystem models (Goulden et al., 2011). Process models require evaluation on how source/sink  
8 transition and long-term carbon flux dynamics respond to differences in vegetation type, harvest  
9 intensity, and age since clearing.

10         Although using the chronosequence approach to evaluate the changes of ecological  
11 processes with age after disturbances is attractive, this approach is often limited by the lack of  
12 biological and climatic data (Yanai et al., 2003; Bond-Lamberty et al., 2006) and full  
13 representation of stand development stages. Process-based ecosystem models provide a means of  
14 quantifying the effects of disturbances on C dynamics under changing climate over various  
15 spatial and temporal scales. Ecosystem models have been used to assess the effects of clearcuts  
16 and climate change on forest C dynamics at the stand/ecosystem (e.g., Bond-Lamberty et al.,  
17 2006; Grant et al., 2009; Wang et al., 2012b) or regional scales (Desai et al., 2007; Dangal et al.,  
18 2014). Moreover, ecosystem models can also be used to assess forest C dynamics under various  
19 scenarios of climate change and harvesting regimes (e.g., Albani et al., 2006; Peckham et al.,  
20 2012), since these models have been developed based on physiological, biogeochemical, and  
21 ecological theories. However, few studies have used ecosystem models to examine the changes  
22 of C fluxes and stocks with stand regrowth after stand-replacing disturbances for forest  
23 chronosequences.

24         The objectives of this study were to evaluate the ability of an ecosystem model to capture  
25 the trajectories of forest C dynamics after stand-replacing harvests for two northern temperate  
26 plant function types (PFTs: deciduous broadleaf forests, DBF; evergreen needleleaf forests,  
27 ENF), to examine which processes influence successional trajectories in these ecosystems, and to  
28 test the role of plant function type on successional trajectory of C fluxes. We applied a process-  
29 based forest ecosystem model, PnET-CN (Aber et al., 1997; Ollinger et al., 2002), to simulate  
30 the effects of clearcut on forest C dynamics, and evaluated the simulated C fluxes and stocks for  
31 both PFTs using in-situ measurements (e.g., eddy covariance observations and aboveground

1 biomass C, AGC). We hypothesized that (1) both DBF and ENF will have similar successional  
2 patterns in C fluxes (GPP, ER, and NEP) and aboveground biomass C stocks after stand-  
3 replacing harvests, but (2) DBF will recover faster than ENF from a net C source to a net C sink  
4 and lose a smaller amount of C (negative NEP) following a stand-replacing harvest.

## 5 **2 Methods**

### 6 **2.1 Study sites and data**

7 Our study sites consist of 8 eddy covariance sites in the Upper Midwest region of  
8 northern Wisconsin and Michigan (Chen et al., 2008; Table 1). The study area is characterized  
9 by a humid-continental climate with hot summers and cold winters. The mean annual  
10 temperature is 4.4 °C and the mean annual precipitation is 768.9 mm (as measured between 1981  
11 and 2010 at Rest Lake weather station, 46.12° N 89.87° W, <http://www.ncdc.noaa.gov>). The  
12 dominant soil type is glacial sandy loam and loamy tills (Noormets et al., 2008). The region has  
13 been strongly influenced by forest industry. Most forest stands less than 100 years old in this  
14 region regenerated following harvesting operations (Amiro et al., 2010).

15 Our sites consist of four DBF sites (YHW, IHW, WIC, and UMBS) and four ENF sites  
16 (YRP, YJP, IRP, and MRP). The four DBF sites range from 3 to 86 years in age and constitute a  
17 chronosequence. Dominant tree species are maple (*Acer* spp.), basswood (*Tilia americana*), birch  
18 (*Betula allghaniensis*), ash (*Fraxinus* spp.) and aspen (*Populus tremuloides*). The four ENF sites  
19 also represent a chronosequence with stand age ranging from 8 to 66 years. Red pine and jack  
20 pine (*Pinus banksiana*) are dominant tree species in the four ENF sites. The two  
21 chronosequences, most sites were initiated by stand-replacing harvests. We obtained monthly C  
22 fluxes (observed NEP and its inferred data products GPP and ER) from AmeriFlux  
23 (<http://public.ornl.gov/ameriflux/>) for the eight eddy covariance flux tower sites (Table 1).  
24 Harmonized level 4 data were used in this study. These flux data have been described and used  
25 in our previous studies (e.g., Noormets et al., 2007; Chen et al., 2008; Desai et al., 2008; Xiao et  
26 al., 2011; Xiao et al., 2014). We also obtained LAI and AGC data from the literature for each site  
27 (Table 1).

## 1   **2.2   Model description**

2           The PnET-CN model is a process-based forest ecosystem model that can simulate C,  
3 nitrogen, and water dynamics at monthly time steps. PnET-CN is driven by temperature,  
4 precipitation, photosynthetically active radiation (PAR), wet and dry nitrogen deposition, and  
5 atmospheric CO<sub>2</sub> concentration (Aber and Driscoll, 1997; Aber et al., 1997; Ollinger et al.,  
6 2002). The model has been applied and tested in the USA and Europe for simulating the effects  
7 of climate variability, rising atmospheric CO<sub>2</sub>, ozone pollution, and disturbance on ecosystem  
8 processes and functions (e.g., Aber et al., 2002; Pan et al., 2009; Peters et al., 2013).

9           One of the unique features of PnET-CN is to simulate potential photosynthesis using  
10 foliar nitrogen concentration and light use efficiency in a multilayered canopy (Aber and  
11 Federer, 1992). Photosynthesis is then constrained by air temperature, vapor pressure deficit, and  
12 soil water availability for simulating actual GPP. The effects of elevated CO<sub>2</sub> concentration on  
13 leaf photosynthetic rates are calculated using constant ratios of leaf internal to ambient CO<sub>2</sub>  
14 concentration ( $C_i/C_a$ ) (Ollinger et al., 2002). PnET-CN incorporates a total of seven C pools, five  
15 of which are structural C pools (foliage, woods, fine roots, woody debris, and soil organic  
16 matter) and two of which are non-structural C pools stored in woods and fine roots.  
17 Photosynthetic production is allocated to each living plant component (i.e., foliage, woods, and  
18 fine roots) and to growth and maintenance respiration. Living biomass is transferred to dead  
19 woody biomass and/or to soil organic C through leaf and root turnover, tree mortality, and  
20 disturbance. The decomposition of coarse woody debris is a constant fraction of its C content.  
21 The decomposition of soil organic C is calculated as a function of maximum decomposition rate  
22 and effects of temperature and soil moisture.

23           PnET-CN includes a complete nitrogen cycle, and simulates nitrogen mineralization and  
24 nitrification, plant nitrogen uptake, allocation, and leaching losses. Nitrogen depositions are  
25 imposed into corresponding soil nitrogen pools (NH<sub>4</sub> and NO<sub>3</sub>). As with C pools, nitrogen is  
26 divided into five structural pools (foliage, woods, fine roots, woody debris, and soil organic  
27 matter) and one non-structural nitrogen pool stored in the trees. C and nitrogen cycles interact  
28 closely in the model. High leaf nitrogen concentration increases net photosynthesis rate in the  
29 absence of water stress, thereby resulting in the high demand for non-structural nitrogen in plant  
30 tissues (Aber et al., 1997). When plant non-structural nitrogen is low, plant nitrogen uptake

1 efficiency from available soil mineral nitrogen is increased in the model (Aber et al., 1997). In  
2 addition, high C: N ratios in biomass, litter, and soil organic matter reduce net mineralization  
3 rates. In general, the nitrogen cycle in the model is governed by a negative feedback loop.

4 The model also simulates key hydrological processes including rainfall interception,  
5 evaporation, transpiration, surface runoff, and drainage at each time step. Rainfall interception is  
6 treated as a constant fraction of precipitation. Transpiration is estimated based on water use  
7 efficiency. Surface runoff is calculated as a constant fraction of the difference between  
8 precipitation and evaporation. Drainage is estimated when potential soil water exceeds soil water  
9 holding capacity.

10 Prescribed disturbance events can be simulated in the model through four parameters:  
11 disturbance year, disturbance intensity, biomass removal fraction, and the loss rate of soil  
12 organic matter. In this study, when stand-replacing disturbance events occur, a uniform plant  
13 function type was assumed to be regenerated on-site. For the first year after clearcuts, minimum  
14 leaf area index (LAI) of 0.1 was assumed to regulate maximum potential foliage mass that  
15 controls leaf production. The photosynthetic production is transported to plant non-structural C  
16 pool where C could be allocated to leaves, stems, and roots. There is therefore no need for  
17 initialization (e.g., stand density) after disturbances in the model. More details about the model  
18 structure and processes have been described elsewhere (Aber et al., 1997; Ollinger et al., 2002).

### 19 **2.3 Model inputs**

20 The model inputs include temperature, precipitation, PAR, wet and dry nitrogen  
21 deposition, atmospheric CO<sub>2</sub> concentrations, and disturbance history. The climate data used in all  
22 simulations were derived from the Daymet database (Thornton et al., 2012). For each site,  
23 monthly maximum temperature, minimum air temperature, and precipitation were calculated  
24 from the daily Daymet data for the period 1981-2010. PAR (mol m<sup>-2</sup> s<sup>-1</sup>) was estimated from  
25 solar radiation (RAD, MJ m<sup>-2</sup> day<sup>-1</sup>) using the empirical relationship (PAR = 2.05 RAD) (Aber et  
26 al., 1996). The data from 1981 to 2010 were repeated as needed to create the time series from  
27 1850 to 1980.

28 Annual rates of wet and dry nitrogen deposition were obtained from the United States  
29 Environmental Protection Agency (EPA; <http://java.epa.gov/castnet/clearsession.do>). The  
30 nitrogen deposition rates were measured at the Wellston station (44.22° N; 85.82° W) for the

1 period 1994-2011. We also obtained the nitrogen deposition rates in 1860 estimated by Galloway  
2 et al. (2004). For each year prior to 1994, we used an exponential ramp function to estimate the  
3 annual deposition rates by interpolating the historical (1860) and current nitrogen deposition  
4 rates. Monthly wet deposition rates, needed for the model, were generated from annual wet  
5 nitrogen deposition through the weighted coefficients (the ratio of monthly precipitation to total  
6 precipitation from March to November). We assumed that there is no wet nitrogen deposition in  
7 the winter. The soil water holding capacity in the rooting zone (100 cm) for each site was derived  
8 from the gridded multi-layer soil characteristics dataset (STATSGO, Miller and White, 1998).  
9 For the period 1959-2010, we used the CO<sub>2</sub> concentrations data from Mauna Loa. For the time  
10 period 1901–1958, we derived the time series of the historical atmospheric CO<sub>2</sub> mixing ratio  
11 using a spline fit to the ice-core record (Etheridge et al., 1996), as described by McGuire et al.  
12 (2001) and used by Xiao et al. (2009). We used the CO<sub>2</sub> concentration in 1901 for the simulation  
13 period prior to 1901 and spin up.

14 For each site, we prescribed the disturbance events using the site disturbance history  
15 (Table 1). For each stand-replacing harvest, stand mortality was assumed to be 100%. The  
16 merchantable wood removal (biomass removal out of the ecosystem) fraction was assumed to be  
17 0.8 in this study. The soil removal fraction was assumed to be zero, given that the content of soil  
18 organic C might not be considerably affected by harvesting (Johnson and Curtis, 2001; Yanai et  
19 al., 2003). We also conducted a sensitivity analysis to these assumptions as described below in  
20 section 2.4.

## 21 **2.4 Parameterization, initialization, validation, and sensitivity analysis**

22 PnET-CN has been parameterized and tested for temperate DBF (Aber et al., 1997;  
23 Ollinger et al., 2002; Peters et al., 2013), temperate ENF (Aber et al., 1997; Peters et al., 2013),  
24 and mixed forests (Aber et al., 1997) for forest productivity, net nitrogen mineralization, and  
25 foliar nitrogen concentrations. The parameter values used in this study are given in supplement  
26 Table S1. To apply the model to the transient simulation period (1860-2010), a 200-year spin up  
27 run was conducted to ensure that the equilibrium ( $\Delta$  NEP < 10 g m<sup>-2</sup> month<sup>-1</sup> and  $\Delta$  soil organic C  
28 < 1%) was reached for each chronosequence site. The climate normals (1981-2010), pre-industry  
29 nitrogen deposition rates, and historical CO<sub>2</sub> concentrations were used for the spin up runs.



1 To examine the stand-replacing harvest legacies, we conducted all simulations using the  
 2 site disturbance history (Table 1), vegetation parameters (Supplement Table S1), climate,  
 3 nitrogen deposition, and atmospheric CO<sub>2</sub> for each of the chronosequence sites. The model  
 4 simulations were evaluated against C fluxes (GPP, ER, and NEP), AGC, and LAI data collected  
 5 at the eddy covariance flux sites. We used two statistical measures to evaluate the overall model  
 6 performance: the normalized root mean square error (NRMSE) and the Willmott index of  
 7 agreement. The NRMSE (Eq. (1)) was used to assess the difference between predicted (*P*) and  
 8 observed (*O*) variables, and can be expressed as:

$$9 \quad \mathbf{NRMSE} = (\mathbf{O}_{max} - \mathbf{O}_{min})^{-1} \left[ \frac{\sum_{i=1}^n (P_i - O_i)^2}{n} \right]^{0.5} \times \mathbf{100\%} \quad (1)$$

10 where *O*<sub>max</sub> and *O*<sub>min</sub> are the maximum and minimum observed values, respectively; *i* is the *i*<sup>th</sup>  
 11 observation; and *n* is the total number of observations. A value close to 0 indicates perfect  
 12 agreement and a value of 100% suggests poor agreement. The Willmott index of agreement (*d*) is  
 13 an indicator of modeling efficiency and is expressed as:

$$14 \quad d = 1 - \left[ \frac{\sum_{i=1}^n (P_i - O_i)^2}{\sum_{i=1}^n (|P_i| + |O_i|)^2} \right] \quad (2)$$

15 A value of 1 indicates perfect agreement and a value near 0 indicates weak agreement (Willmott,  
 16 1982).

17 The sensitivity of ecosystem C dynamics to changes in harvesting practices during the  
 18 secondary succession was assessed using sensitivity analysis. The model was run at WIC and  
 19 MRP for 100 years after scenario harvests in 1910 using the same climate data sequence.  
 20 Sensitivity scenarios involved applying the stand mortality (80% and 60%, compare to 100% in  
 21 the model test), soil organic matter loss (20% and 40%, compare to zero in the model test) to  
 22 reveal effects of different harvest intensity and soil organic matter loss scenarios on C dynamics.  
 23 We also tested the model sensitivity to CO<sub>2</sub> fertilization for evaluating potential climate change  
 24 effects.

25

## 1 **3 Results**

### 2 **3.1 Evaluation of modeled carbon fluxes and stocks**

3 The simulated C fluxes were generally consistent with eddy covariance derived C fluxes  
4 for both DBF and ENF sites (Figs. 1 and 2). The NRMSE between simulated and tower fluxes  
5 (GPP, ER, and NEP) were between 10-21% (Table 2). The Willmott index of agreement between  
6 simulated and tower C fluxes for both plant function types ranged from 0.91 to 0.94 with the  
7 exception of NEP ( $d= 0.73$ ,  $n= 235$ ). The model underestimated GPP for the DBF sites and  
8 predicted ER fairly well for all DBF sites except for the intermediate-aged hardwood site, IHW.  
9 As a result, the model underestimated NEP for most DBF sites. For IHW, the model substantially  
10 underestimated both GPP and ER but predicted NEP fairly well. For the ENF sites, the model  
11 underestimated GPP. The model predicted ER fairly well for YRP (8 years old), YJP (15-16  
12 years old) and IRP (23 years old), but overestimated ER for the older MRP sites. Thus, the model  
13 underestimated NEP for the ENF sites.

14 The simulated and observed stand characteristics (LAI and AGC) showed good  
15 agreement (Table 2 and Fig. 3). The model slightly underestimated LAI for the young forest sites,  
16 and overestimated LAI for the mature forest sites. Generally, the model overestimated AGC for  
17 the mature forest sites. The NRMSE was 28% for AGC and 31% for LAI. The Willmott index of  
18 agreement was 0.95 and 0.96 for AGC and LAI, respectively. Overall, the model evaluation  
19 metrics indicated that the model performed better in the DBF sites than in the ENF sites.

### 20 **3.2 Legacy of clearcut on carbon fluxes and stocks**

21 PnET-CN generally captured the changes of C fluxes following the clearcuts for each  
22 chronosequence site (Fig. 4). The predicted annual GPP generally increased with time since  
23 disturbance and approached the peak values ( $\sim 1200\text{--}1500 \text{ g C m}^{-2} \text{ yr}^{-1}$ ) between 11 and 26 years  
24 of age and between 29 and 30 years of age for the DBF (IHW, WIC, and UMBS) and the ENF  
25 (IRP and MRP) sites, respectively; thereafter, the forest stands reached maturity and GPP  
26 became relatively stable with mean values of  $940\text{--}1000 \text{ g C m}^{-2} \text{ yr}^{-1}$ .

27 Predicted annual ER was initially as high as  $860\text{--}1030$  and  $710\text{--}860 \text{ g C m}^{-2} \text{ yr}^{-1}$  within  
28 the first two years for the DBF and the ENF sites, respectively. During canopy recovery,  
29 predicted ER generally decreased to  $620\text{--}780 \text{ g C m}^{-2} \text{ yr}^{-1}$  between 10 and 25 years of age for the

1 DBF sites and to 360–380 g C m<sup>-2</sup> yr<sup>-1</sup> between 14 and 17 years of age for the ENF sites (Fig. 4).  
2 For forest age older than 60 years, the predicted annual ER for both PFTs showed a relatively flat  
3 pattern, contrary to theoretical expectations, arising from the little change of both autotrophic  
4 and heterotrophic respiration with age (Supplement Fig. S1). Average annual ER for mature  
5 forests was 810–880 and 780 g C m<sup>-2</sup> yr<sup>-1</sup> for the DBF sites (WIC and UMBS) and the ENF  
6 (MRP) site, respectively.

7 As expected, the ratio of annual GPP to annual ER (GPP: ER) simulated by PnET-CN  
8 was low during the early years after clearcutting for both DBF and ENF (Fig. 5). Within ~6 years  
9 for the DBF sites and ~17 years for the ENF sites, the GPP:ER ratio gradually increased and its  
10 average value became larger than 1 (NEP>0). The simulated peak GPP:ER ratio for DBF (1.6)  
11 occurred at 18 years after stand-replacing harvests, and the simulated peak ratio for ENF was 1.8  
12 at 26 years. After those peaks, the ratio became relatively stable, with the mean values of 1.1 and  
13 1.2 for mature DBF and mature ENF, respectively.

14 The model predicted negative NEP (C source) for the 6 and 17 years after stand-replacing  
15 harvests for the DBF and the ENF, respectively (Fig. 4). The simulated peak annual net C loss  
16 occurred in the first or second year after clearcutting. The average C loss was 530–710 g C m<sup>-2</sup>  
17 yr<sup>-1</sup> for the DBF sites and 380–400 g C m<sup>-2</sup> yr<sup>-1</sup> for the ENF sites. The total C loss was 3.2–4.3  
18 and 6.4–6.9 kg C m<sup>-2</sup> for the DBF and the ENF sites, respectively. The maximum net C gain was  
19 387–433 g C m<sup>-2</sup> yr<sup>-1</sup> at 14–26 years of age for the DBF sites (WIC and UMBS) and was 567–  
20 602 g C m<sup>-2</sup> yr<sup>-1</sup> at 29 years of age for the ENF sites (IRP and MRP). Simulated annual NEP  
21 decreased thereafter and became as low as 120–180 g C m<sup>-2</sup> yr<sup>-1</sup> after 17–31 years for the DBF  
22 sites and 170 g C m<sup>-2</sup> yr<sup>-1</sup> after 44 years for the ENF sites.

23 Forest canopy as measured by LAI gradually recovered over time following clearcuts  
24 (Fig. 6). LAI fully recovered within 10–15 years after disturbance for the DBF sites and within  
25 40 years of age for the ENF sites. The gradual recovery of LAI led to the gradual increase in  
26 GPP and the subsequent increase in AGC (Fig. 7). In general, AGC recovered much more slowly  
27 than C fluxes and LAI. The changes of simulated AGC followed the logistic growth curve with  
28 slow accumulation in the early years, fast accumulation in the middle age, and slow  
29 accumulation afterwards. The predicted LAI and AGC generally fell within the range of  
30 observed values across two chronosequences (Figs. 3, 6, 7). For mature forests (>60 years of

1 age) in 2010, the DBF sites generally stored more C in aboveground biomass than the ENF sites  
2 (10–12 vs. 8.5 kg C m<sup>-2</sup>; Fig. 7).

### 3 **3.3 Sensitivity analysis**

4 Harvest intensity had little effect on the long-term C dynamics for both PFTs, but it had  
5 sizeable effects during early succession (Fig. 8). Greater harvest intensity led to earlier rising  
6 GPP (Fig. 8 a and f) and LAI (Fig. 8 d and i) but delayed reduction in ER (Fig. 8 b and g),  
7 resulting in later rising NEP (Fig. 8 c and g). High harvest intensity (e.g., 100% removal of living  
8 trees) also directly reduced living tree AGC (Fig. 8 e and i). By reducing harvest intensity  
9 parameter to 80% and 60% from 100% used in the original model, average annual NEP over 100  
10 years for DBF decreased by 104 and 88 g C m<sup>-2</sup> yr<sup>-1</sup>, respectively. The increased remaining tree  
11 biomass resulted in an increase in AGC about 12% and 16%, respectively, after a 100-yr harvest  
12 cycle. For ENF average annual NEP decreased about 1% and AGC decreased nearly 6% for both  
13 reduced harvest intensity scenarios. Increasing soil removal fraction parameter resulted in lower  
14 GPP and ER along succession and lower NEP in middle succession for both DBF and ENF (Fig.  
15 S2 a-c and f-h). Greater soil removal fraction promoted the leaf production of DBF in middle and  
16 late succession (Fig. S2 d), but restricted the leaf production of ENF in late succession (Fig.S2 i).  
17 Increasing soil removal fraction parameter (20% and 40% removal of soil organic matter)  
18 strongly reduced living AGC (16% and 39%, respectively) for DBF (Fig. S2 e) but slightly  
19 decrease living AGC (up to 5%) for ENF (Fig. S2 j). There were little effects of CO<sub>2</sub> fertilization  
20 on carbon dynamics for both DBF and ENF in our sensitivity analysis (Fig. S3).

## 21 **4 Discussion**

### 22 **4.1 Carbon fluxes and stocks following clearcuts**

23 PnET-CN generally simulated the expected post-harvest trajectories in C fluxes (GPP,  
24 ER, and NEP) and stock (LAI and AGC). The model was unable to simulate high GPP rates  
25 estimated by eddy covariance in mature forests regardless of vegetation type, suggesting that  
26 there is room for improvement in model simulation of secondary succession.

27 Our simulations showed that LAI increased rapidly first and then stabilized during the  
28 following development stages, given that the model estimates foliage growth through the  
29 parameter of maximum relative growth rate (Table S1) with the limitation of current foliage

1 biomass and resource availability. This modeled response is consistent with the previous finding  
2 that foliage biomass increased rapidly after disturbance and then stabilized (Sprugel 1985). Our  
3 chronosequence-based results are generally consistent with previous results. For example,  
4 Goulden et al. (2011) observed that LAI along a chronosequence of boreal forest stands  
5 increased rapidly from  $0.3 \text{ m}^2 \text{ m}^{-2}$  1 year after fire, and then generally leveled off at  $5.3\text{--}7.2 \text{ m}^2$   
6  $\text{m}^{-2}$  from 23 to 154 years after stand-replacing crown fire. A modeling study based on a modified  
7 version of Biome-BGC (Bond-Lamberty et al., 2005) also showed a similar successional change  
8 in LAI for boreal DBF and ENF.

9         The simulated successional change in annual GPP for both PFTs generally followed the  
10 trajectory hypothesized by Odum (1969). However, despite a slight decrease in GPP  
11 hypothesized in Odum's trajectories, our simulations show a relatively flat GPP in mature forests  
12 (Figs. 4 and 10). In the model, GPP tracks LAI in the absence of significant changes in light,  
13 water or nutrient stress. As LAI stabilizes in mature forests, GPP also stabilizes. Our results are  
14 consistent with previous studies showing relatively flat pattern in GPP after 20 years following  
15 harvests in temperate pine forests in Florida (Clark et al., 2004), northern temperate DBF in  
16 Wisconsin (Desai et al., 2008), and boreal jack pine forests in Saskatchewan (Zha et al., 2009).  
17 Furthermore, Humphreys et al. (2006) reported continuous increases of GPP with increasing  
18 forest age for temperate rainforests using three different stands at different stages of development  
19 (2, 14, and 53 years of age) following clearcuts in British Columbia, Canada. However, northern  
20 temperate ENF showed a small difference in GPP between young and mature sites (Noormets et  
21 al., 2007; Desai et al., 2008). Desai et al. (2005) found that a nearby old-growth mixed forest had  
22 slightly lower GPP and significantly higher ER than nearby DBF sites. Site-to-site variations in  
23 species and soil fertility could result in variations in the successional trajectory of GPP after  
24 clearcuts so that the observed trajectories may deviate from hypothesized or modeled  
25 trajectories. In addition, our chronosequences lack old-growth sites and do not encompass the  
26 full range of forest development stages, which limits the representativeness of the C flux and  
27 stock trajectories derived from chronosequence studies based on eddy covariance or other  
28 ecological observations (e.g., Clark et al., 2004; Humphreys et al., 2006; Noormets et al., 2007).

29         Our simulations show that annual ER for secondary temperate forests slightly declined in  
30 the first ten years because of low autotrophic respiration at first after the removal of trees. Amiro  
31 et al. (2010) reported that ER reduced in the very first year following harvests for a number of

1 eddy covariance flux sites over North America. Previous field studies showed that ER following  
2 clearcuts increased with forest age (e.g., Humphreys et al., 2006; Zha et al., 2009), partly  
3 supporting our results that ER slightly increased after the short decline period (10-25 years of  
4 age) in northern temperate forests until the stands reached maturity. Martin and Bolstad (2005)  
5 showed that chamber-based soil respiration in DBF of northern Wisconsin ranged from 857–  
6 1143 g C m<sup>-2</sup> yr<sup>-1</sup> in 1998 and 1013–1357 g C m<sup>-2</sup> yr<sup>-1</sup> in 1999, which is higher than tower ER  
7 (825±133 g C m<sup>-2</sup> yr<sup>-1</sup>, WIC) from 1999-2006 in the same region. Soil respiration of 690 g C m<sup>-2</sup>  
8 over the growing season of 2005 in a mature DBF near WIC tower site was reported (Tang et al.,  
9 2009). Our simulated respiration components (e.g., soil respiration) for DBF were lower than  
10 those reported values (Supplement Fig. S1). The model underestimated GPP but estimated ER  
11 well for mature DBF sites, indicating that the model likely overestimated root autotrophic  
12 respiration. Eddy covariance derived ER were usually lower than chamber-based estimate at the  
13 WIC site due to uncertainties induced by measurement methods, decoupling of surface and  
14 canopy fluxes at night, and spatial scaling (Bolstad et al., 2004; Cook et al., 2004). For ENF, the  
15 model overestimated ER for the mature site because of overestimated soil decomposition rate.  
16 Our simulations also show that DBF had slightly higher soil respiration rate than ENF  
17 (Supplement Fig. S1), which is consistent with the finding that chamber-based soil respiration  
18 was slightly higher for DBF than for ENF (no significant difference) in Wisconsin (Euskirchen et  
19 al., 2003). The changes of ER in secondary forests after clearcutting differ among sites because  
20 of different site conditions (e.g., quantity and quality of soil organic C and litter C) and  
21 harvesting types (e.g., Tang et al., 2009).

22         The trajectory of our simulated GPP: ER ratio is similar to the curve derived by Amiro et  
23 al. (2010) using EC observations and forest age from fire and harvest chronosequences across  
24 North America (GPP: ER = 1.23\*[1-exp(-0.224\*AGE)]). Our simulated ratios are within the  
25 observed range of 0.9–1.6 for the DBF sites (Fig. 5a), although the model underestimated the  
26 ratios for mature sites. The growing season GPP :ER ratios are typically higher than the annual  
27 ratios because winter soil organic C decomposition is important to annual C balance (Aanderud  
28 et al., 2013). However, the simulated ratios for the ENF sites are much lower than tower-derived  
29 growth season ratios (1.9–4.7, Fig. 5b), and close to the annual range of 1.6–2.2 estimated by  
30 Desai et al. (2008). The standard gap-filling methods of the eddy covariance flux data may lead

1 to the overestimation of net ecosystem exchange due to the lack of winter C flux observations for  
2 the ENF sites and two of the DBF sites (YHW and IHW).

3 Our simulated successional dynamics of NEP following clearcuts generally supported the  
4 trajectory hypothesized by Odum (1969) and Chapin et al. (2002). The similar trajectories,  
5 however, were caused by different reasons. Odum's trajectories show declining GPP and  
6 relatively flat community respiration with time. Our simulated decline in NEP resulted from  
7 relatively flat GPP and growing ER with stand development (Figs. 4 and 8). This has been  
8 observed for northern temperate hardwood chronosequence sites (Desai et al., 2008), northern  
9 temperate pine forests (Peichl et al. 2010), and boreal DBF forests (e.g., Goulden et al., 2011). A  
10 recent North American Carbon Program (NACP) synthesis study showed similar changes in NEP  
11 after either stand-replacing fire or harvest based on eddy covariance chronosequence  
12 measurements across North America (Amiro et al., 2010).

13 Chapin et al. (2002) hypothesized that heterotrophic respiration is initially high, declines  
14 in middle succession, and rises thereafter, while NPP reaches a peak in middle age and declines  
15 in old stands. The simulated successional trajectories in heterotrophic respiration support the  
16 pattern hypothesized by Chapin et al. (2002), whereas our simulated NPP did not decline in  
17 mature stands (Supplement Fig. S1). Previous studies also support our simulated trajectory in  
18 heterotrophic respiration. For example, Pregitzer and Euskirchen (2004) reported that  
19 heterotrophic respiration was high (mean value of  $970 \text{ g C m}^{-2} \text{ yr}^{-1}$ ) in young temperate forests,  
20 declined with age in middle succession, and increased with time for mature forests, although for  
21 old temperate forests (>120 years) the decline in NPP reduced heterotrophic respiration. The  
22 decline of NPP with age was not predicted in this study. Validation of the simulated NPP was not  
23 possible in this study due to the lack of NPP measurements across all sites. Our simulated  
24 heterotrophic respiration for mature DBF is close to the observation of  $502 \pm 86 \text{ g C m}^{-2} \text{ yr}^{-1}$  in a  
25 mature DBF near UMBS tower site between 1999 and 2003 (Gough et al., 2008). However, ENF  
26 chronosequence sites in this study show that NEP continually increased with age because of  
27 relatively flat and low ER ( $340 \pm 96 \text{ g C m}^{-2} \text{ yr}^{-1}$ ) and increasing GPP. Successional changes in C  
28 fluxes after fire and harvest are similar over chronosequence sites of North America (Amiro et  
29 al., 2010), although a specific chronosequence study in Saskatchewan, Canada, observed that C  
30 fluxes are greater at the burned site than the harvested sites (Mkhabela et al., 2009).

1           Although our model underestimated NEP and GPP for both the DBF and ENF sites in the  
2 Upper Midwest region (Figs.1 and 2), our predicted NEP was comparable to estimates from  
3 other studies in similar regions. For example, our predicted maximum NEP for the ENF sites  
4 (567–602 g C m<sup>-2</sup> yr<sup>-1</sup>, 29 years of age) was slightly lower than the estimates (690 g C m<sup>-2</sup> yr<sup>-1</sup>,  
5 15–20 years of age) for afforested white pine (*Pinus strobus*) forests in Ontario (Coursolle et al.,  
6 2012). For a northern temperate forest chronosequence study in northern Michigan, NEP higher  
7 than 200 g C m<sup>-2</sup> yr<sup>-1</sup> in young DBF forests could be derived from the reference forest (153± 115  
8 g C m<sup>-2</sup> yr<sup>-1</sup>, 85 years of age) (Gough et al., 2007), suggesting that our predictions (390–430 g C  
9 m<sup>-2</sup> yr<sup>-1</sup>, 14–26 years of age) for the DBF sites could be in the reasonable range. Furthermore, our  
10 predicted mean annual NEP (123–177 g C m<sup>-2</sup> yr<sup>-1</sup>) for mature DBF sites (>60 years) was close  
11 to estimates for other northern DBF, including a northern hardwood forest of central  
12 Massachusetts (200±40 g C m<sup>-2</sup> yr<sup>-1</sup>, Barford et al., 2001) and four eastern North American DBF  
13 (167-236 g C m<sup>-2</sup> yr<sup>-1</sup> Curtis et al., 2002).

14           We found that the simulated AGC during forest regrowth gradually increased following  
15 the typical logistic growth curve (Sprugel, 1985). In the model, low NPP in the early stages  
16 results in slow AGC accumulation. Once the amount of NPP approximately equals annual dead  
17 biomass C that is largely controlled by the wood turnover rate, the trajectory of AGC reaches a  
18 plateau. Previous chronosequence studies showed that AGC increased with increasing age (e.g.,  
19 Peichl and Arain, 2006; Goulden et al., 2011; Powers et al., 2012). Powers et al. (2012) reported  
20 that AGC increased rapidly with age in young red pine stands across a chronosequence in  
21 northern Minnesota, USA. The representativeness and generalization of these findings were  
22 limited by the small number of young stands (Powers et al., 2012).

23           Sensitivity analysis shows that more intensive harvests could have larger and longer  
24 impacts on successional trajectories of C dynamics in early succession for both DBF and ENF.  
25 Fewer flux tower based studies have investigated the effects of harvest intensity on forest C  
26 fluxes (e.g., GPP, ER, and NEP) because of the high establishment cost of eddy covariance  
27 system. Nevertheless, some modeling studies have provided insights into how forest C fluxes  
28 and stocks are affected by harvest intensity. Our findings are supported by previous modeling  
29 studies. For example, a recent modeling study of temperate forests reported that more intensive  
30 harvests increased the recovery time of NPP for ENF and DBF in Minnesota and Wisconsin,  
31 USA (Peters et al. 2013). In the boreal forest of central Canada less intensive harvest and longer



1 rotation length might increase total C sink (sum of biomass C and soil organic C) up to 40%  
2 (Peng et al. 2002), although recent studies indicate that longer rotation length could not  
3 necessarily increase C sequestration under changing climate conditions (Wang et al., 2012b;  
4 Wang et al., 2013). If harvesting operations largely reduce soil organic matter, C fluxes (e.g.,  
5 GPP, NPP, ER, and NEP) and living AGC are reduced for both PFTs. Consistent with this,  
6 Peters et al. (2013) showed that simulated NPP could not recover to pre-harvesting levels due to  
7 greater removal of soil organic matter. Therefore, our model results suggest management  
8 practices should aim to decrease soil disturbance caused by harvest operations.

#### 9 **4.2 Differences between DBF and ENF**

10 Our results showed that DBF may reach a peak in LAI and GPP faster than ENF after  
11 clearcutting, showing clear differences in pattern of ecosystem development between the DBF  
12 and ENF sites. More rapid recovery of LAI and GPP for DBF sites lead to sooner recovery of  
13 NEP and AGC regardless of harvest intensity, supporting our second hypothesis. The foliage  
14 related parameters such as FolRelGroMax and AmaxB mainly govern the differences in  
15 successional trajectories between the two PFTs (Supplement Table S1). DBF is assumed to have  
16 more productive foliage than ENF, and more photosynthetic production then can lead to more  
17 foliage production. With this positive feedback in the model, GPP, NEP, and AGC of the DBF  
18 sites recover more rapidly than those of the ENF sites. Our findings are consistent with the  
19 chronosequence studies showing that the temperate DBF in northern Michigan rapidly became a  
20 net C sink after six years following disturbances (Gough et al., 2007) and that ENF stands in  
21 northern Wisconsin became net C sinks within 10-15 years after harvesting (Noormets et al.,  
22 2007). Through the analysis of the Forest Inventory and Analysis (FIA) data, Williams et al.  
23 (2012) suggested that faster growth in AGC at high productivity sites caused higher C fluxes and  
24 stocks. Our findings are also consistent with a recent modeling study suggesting that temperate  
25 DBF switches to positive NEP faster than temperate ENF after clearcuts, and DBF has a higher  
26 peak in NEP compared to ENF (Peckham et al., 2012). A modeling study conducted in boreal  
27 forests also reported that low productive boreal ENF needed 1-3 more years to attain a positive  
28 NEP than boreal DBF after clearcuts in Saskatchewan, Canada (Wang et al., 2012b). These  
29 observed and modeled successional changes further indicate that DBF tend to have higher  
30 photosynthetic capacity than ENF in the early stage of stand development following stand-  
31 replacing harvests.

1           The sensitivity analysis suggests that more productive forests could be more strongly  
2 affected by greater soil removal fraction, as soil removal reduces soil organic matter thereby  
3 resulting in relatively low nitrogen mineralization in the model. Peters et al (2013) showed that  
4 NPP was more strongly reduced for Aspen than for jack pine in their simulations. However,  
5 productive lodgepole pine (*Pinus contorta* Dougl. ex Loud.) could maintain high productivity at  
6 12 years after harvest disturbance regardless of soil organic carbon removal and soil compaction  
7 treatments because beneficial ectomycorrhizal fungi associated with lodgepole pine could help  
8 access nitrogen from organic matter; while hybrid white spruce (*Picea glauca* × *engelmannii*  
9 [Moench] Voss) was more sensitive to the treatments (Kranabetter et al., 2006). The discrepancy  
10 might be caused by the lack of representation of relationship between fungi and plants in the  
11 model.

### 12 **4.3 Limitations and challenges**

13           PnET-CN can explicitly simulate the effects of disturbance, pollution, and climate change  
14 on forest C dynamics (e.g., Ollinger et al., 2002; Pan et al., 2009; Peters et al., 2013). Despite the  
15 capability of the model, we do recognize that the model has some limitations in simulating  
16 harvesting effects, and that the accurate representation of the trajectories of C fluxes and stocks  
17 following harvests still remains a challenge.

18           First, the performance of the model to simulate forest regrowth after harvests is limited  
19 by the absence of regeneration and understory in the model. Most process-based models such as  
20 PnET-CN and TEM (Raich et al., 1991) have been mainly developed to simulate C balance for  
21 mature forests over the past decades (Landsberg, 2003), resulting in no provision for simulating  
22 regeneration such as shrub component and species succession in these models. Changes in forest  
23 composition (e.g., evergreen and deciduous tree species and understory shrubs) along the course  
24 of succession are not fully considered by most ecosystem models. PnET-CN does not simulate  
25 shrubs and herbs that likely dominate stands in the early successional stage after stand-replacing  
26 harvests. Therefore, the model is not able to simulate the particularly high GPP and ER in the  
27 young forests where forest canopy has not yet fully recovered.

28           Understory layer is also an important component for mature forest ecosystems in terms of  
29 C fluxes (Misson et al., 2007) and stocks. Misson et al. (2007) reported that understory can  
30 contribute 11% (range, 0–39%) of GPP at 10 sites across a wide range of forest type and climate.

1 PnET-CN slightly overestimated overstory LAI for the mature DBF sites and reasonably  
2 predicted foliar nitrogen concentration compared to satellite-based estimates (data not shown).  
3 The lack of understory layer in the model is possibly responsible for the underestimation of GPP  
4 for mature DBF sites. Species competition and cohort methods that have been employed in other  
5 models such as ED (Medvigy et al., 2009) and LPG-Guess (Smith et al., 2001) could be used to  
6 improve the regeneration and understory components of PnET-CN in the future.

7         Second, parameter values used in the model were generally derived from specific  
8 measurements for a given stand development stage particularly mature forests, although the  
9 parameter values likely differ with stand development. For example, the canopy light attenuation  
10 constant coefficient is typically measured in mature forests (e.g., Ryu et al., 2008), although the  
11 coefficient is known to change with canopy cover (Brantley and Young, 2007). The use of the  
12 canopy light attenuation coefficient measured in mature forest for whole forest life simulations  
13 could slow down stand development due to the underestimation of photosynthesis in young  
14 forests. Understanding the relationship between such parameters and state variables (e.g., LAI) is  
15 thus one of the challenges to simulate the effects of stand-replacing harvests on forest C  
16 dynamics.

17         Third, changing climate conditions can also affect the values of some parameters. For  
18 example, wood turnover rate (%), tree mortality in terms of biomass losses), to which wood living  
19 biomass C and soil organic C are sensitive, could be altered by extreme weather conditions  
20 including droughts (Allen et al., 2010; Wang et al., 2012a). Most process-based models are not  
21 able to simulate the mechanistic processes associated with tree mortality under changing climate  
22 conditions (McDowell, 2011; Wang et al., 2012a), although there is growing interest in the  
23 mechanistic modeling of forest mortality (e.g., McDowell et al., 2013; Powell et al., 2013).  
24 Recent studies have revealed that climate and disturbance legacies govern forest C dynamics  
25 (Magnani et al., 2007; Bond-Lamberty et al., 2013). Future modeling efforts can benefit from  
26 improved understanding of the effects of climate change on parameter values that are assumed to  
27 be constant in the model.

28         Finally, the whole silvicultural system (e.g., harvests) is not fully considered in the  
29 model. Harvest methods depend on forest types, management needs, and species to be  
30 regenerated. For example, selective harvesting or shelterwood system is typically used for

1 hardwoods in Wisconsin (Wisconsin Department of Natural Resources, 2011). Stand-replacing  
2 harvesting was assumed for both DBF and ENF chronosequence sites due to the lack of  
3 harvesting information and the types of clearing applied to the sites studied. The sensitivity  
4 analysis conducted in this study suggests that harvest intensity affects C dynamics in early  
5 succession after harvesting. Observations in residuals and post stands after each operation type  
6 (e.g., pre-commercial thinning and selective harvesting) are needed to parameterize process-  
7 based models for better mechanistic understanding of the harvest effects on forest C dynamics.

8        Besides disturbances, climate is also a key driver of ecosystem structure and function.  
9 Climate extremes such as drought induce forest die-off and reduction of carbon uptake globally  
10 (Ciais et al., 2005; Kurz et al., 2008; van Mantgem et al., 2009; Zhao and Running, 2010; Peng  
11 et al., 2011; Ma et al., 2012; Schwalm et al., 2012). In North America, droughts and disturbance  
12 are two main sources of interannual variability in carbon fluxes (Xiao et al. 2011, 2014). Future  
13 modeling studies should explicitly the effects of both disturbance and climate extremes.

## 14 **5 Conclusions**

15        The PnET-CN model is generally able to simulate the effects of stand-replacing harvests  
16 on forest C dynamics (C fluxes and AGC) for two northern temperate forest chronosequences.  
17 The predicted dynamics in NEP and AGC following clearcuts generally follow the hypothesized  
18 trajectories (Odum, 1969; Chapin et al., 2002), although our simulations show that the decline in  
19 NEP was due to relatively flattening GPP and gradually increasing ER. Our study also shows  
20 that DBF recovered faster (11 years) from net C sources to net sinks and accumulated more C in  
21 AGC than ENF. Northern temperate ENF is more vulnerable to stand-replacing harvests than  
22 northern temperate DBF. Future research is needed to better understand how respiration  
23 components (e.g., ecosystem and soil respiration) and production components (e.g., overstory  
24 and understory) change with forest age and their determinants. Modeling the combined effects of  
25 climate change and forest management will benefit from the incorporation of forest population  
26 dynamics (e.g., regeneration and mortality), relationships between age-related model parameters  
27 and state variables (e.g., LAI), and silvicultural system into the model. With these improvements,  
28 process-based ecosystem models can better simulate regional C balance associated with  
29 disturbance regime under changing climate.

1 **Acknowledgements**

2           This study was supported by National Science Foundation (NSF) through MacroSystems  
3 Biology (award number 1065777; PI: J. Xiao). We thank Lucie Lepine, Zaixing Zhou, Andrew  
4 Ouimette, and Alexandra Thorn for helpful discussion. We also thank the anonymous reviewers  
5 and Peter Curtis for their constructive comments on the manuscript.

6

## 1 **References**

- 2 Aanderud, Z. T., Jones, S. E., Schoolmaster Jr, D. R., Fierer, N., and Lennon, J. T.: Sensitivity of  
3 soil respiration and microbial communities to altered snowfall, *Soil Biology and*  
4 *Biochemistry*, 57, 217-227, 10.1016/j.soilbio.2012.07.022, 2013.
- 5 Aber, J. D., and Federer, C. A.: A generalized, lumped-parameter model of photosynthesis,  
6 evapotranspiration and net primary production in temperate and boreal forest ecosystems,  
7 *Oecologia*, 92, 463-474, 10.1007/bf00317837, 1992.
- 8 Aber, J. D., Reich, P. B., and Goulden, M. L.: Extrapolating leaf CO<sub>2</sub> exchange to the canopy: a  
9 generalized model of forest photosynthesis compared with measurements by eddy correlation,  
10 *Oecologia*, 106, 257-265, 10.1007/bf00328606, 1996.
- 11 Aber, J. D., and Driscoll, C. T.: Effects of land use, climate variation, and N deposition on N  
12 cycling and C storage in northern hardwood forests, *Glob. Biogeochem. Cycle*, 11, 639-648,  
13 1997.
- 14 Aber, J. D., Ollinger, S. V., and Driscoll, C. T.: Modeling nitrogen saturation in forest  
15 ecosystems in response to land use and atmospheric deposition, *Ecol. Model.*, 101, 61-78,  
16 1997.
- 17 Aber, J. D., Ollinger, S. V., Driscoll, C. T., Likens, G. E., Holmes, R. T., Freuder, R. J., and  
18 Goodale, C. L.: Inorganic nitrogen losses from a forested ecosystem in response to physical,  
19 chemical, biotic, and climatic perturbations, *Ecosystems*, 5, 648-658, 2002.
- 20 Albani, M., Medvigy, D., Hurtt, G. C., and Moorcroft, P. R.: The contributions of land-use  
21 change, CO<sub>2</sub> fertilization, and climate variability to the Eastern US carbon sink, *Glob.*  
22 *Change Biol.*, 12, 2370-2390, 10.1111/j.1365-2486.2006.01254.x, 2006.
- 23 Allen, C. D., Macalady, A. K., Chenchouni, H., Bachelet, D., McDowell, N., Vennetier, M.,  
24 Kitzberger, T., Rigling, A., Breshears, D. D., Hogg, E. H., Gonzalez, P., Fensham, R., Zhang,

1 Z., Castro, J., Demidova, N., Lim, J.-H., Allard, G., Running, S. W., Semerci, A., and Cobb,  
2 N.: A global overview of drought and heat-induced tree mortality reveals emerging climate  
3 change risks for forests, *For. Ecol. Manage.*, 259, 660-684, DOI:  
4 10.1016/j.foreco.2009.09.001, 2010.

5 Amiro, B. D., Barr, A. G., Barr, J. G., Black, T. A., Bracho, R., Brown, M., Chen, J., Clark, K.  
6 L., Davis, K. J., Desai, A. R., Dore, S., Engel, V., Fuentes, J. D., Goldstein, A. H., Goulden,  
7 M. L., Kolb, T. E., Lavigne, M. B., Law, B. E., Margolis, H. A., Martin, T., McCaughey, J.  
8 H., Misson, L., Montes-Helu, M., Noormets, A., Randerson, J. T., Starr, G., and Xiao, J.:  
9 Ecosystem carbon dioxide fluxes after disturbance in forests of North America, *J. Geophys.*  
10 *Res.*, 115, G00K02, 10.1029/2010jg001390, 2010.

11 Barford, C. C., Wofsy, S. C., Goulden, M. L., Munger, J. W., Pyle, E. H., Urbanski, S. P.,  
12 Hutyra, L., Saleska, S. R., Fitzjarrald, D., and Moore, K.: Factors Controlling Long- and  
13 Short-Term Sequestration of Atmospheric CO<sub>2</sub> in a Mid-latitude Forest, *Science*, 294, 1688-  
14 1691, 10.1126/science.1062962, 2001.

15 Bolstad, P. V., Davis, K. J., Martin, J., Cook, B. D., and Wang, W.: Component and whole-  
16 system respiration fluxes in northern deciduous forests, *Tree Physiol.*, 24, 493-504, 2004.

17 Bond-Lamberty, B., Gower, S. T., Ahl, D. E., and Thornton, P. E.: Reimplementation of the  
18 Biome-BGC model to simulate successional change, *Tree Physiol.*, 25, 413-424, 2005.

19 Bond-Lamberty, B., Gower, S. T., Goulden, M. L., and McMillan, A.: Simulation of boreal black  
20 spruce chronosequences: Comparison to field measurements and model evaluation, *J.*  
21 *Geophys. Res.*, 111, G02014, 10.1029/2005JG000123, 2006.

1 Bond-Lamberty, B., Rocha, A. V., Calvin, K., Holmes, B., Wang, C., and Goulden, M. L.:  
2 Disturbance legacies and climate jointly drive tree growth and mortality in an intensively  
3 studied boreal forest, *Glob. Change Biol.*, 20, 216-227, 10.1111/gcb.12404, 2013.

4 Brantley, S. T., and Young, D. R.: Leaf-area index and light attenuation in rapidly expanding  
5 shrub thickets, *Ecology*, 88, 524-530, 10.1890/06-0913, 2007.

6 Chapin, F. S., Matson, P. A., and Mooney, H. A.: *Principles of Terrestrial Ecosystem Ecology*,  
7 Springer, New York., 2002.

8 Chen, J., Davis, K. J., and Meyers, T. P.: Ecosystem-atmosphere carbon and water cycling in the  
9 upper Great Lakes Region, *Agric. For. Meteorol.*, 148, 155-157,  
10 10.1016/j.agrformet.2007.08.016, 2008.

11 Ciais, P., Reichstein, M., Viovy, N., Granier, A., Ogee, J., Allard, V., Aubinet, M., Buchmann,  
12 N., Bernhofer, C., Carrara, A., Chevallier, F., De Noblet, N., Friend, A. D., Friedlingstein, P.,  
13 Grunwald, T., Heinesch, B., Keronen, P., Knohl, A., Krinner, G., Loustau, D., Manca, G.,  
14 Matteucci, G., Miglietta, F., Ourcival, J. M., Papale, D., Pilegaard, K., Rambal, S., Seufert,  
15 G., Soussana, J. F., Sanz, M. J., Schulze, E. D., Vesala, T., and Valentini, R.: Europe-wide  
16 reduction in primary productivity caused by the heat and drought in 2003, *Nature*, 437, 529-  
17 533, [http://www.nature.com/nature/journal/v437/n7058/supinfo/nature03972\\_S1.html](http://www.nature.com/nature/journal/v437/n7058/supinfo/nature03972_S1.html), 2005.

18 Clark, K. L., Gholz, H. L., and Castro, M. S.: Carbon dynamics along a chronosequence of slash  
19 pine plantation in north Florida, *Ecol. Appl.*, 14, 1154-1171, 10.1890/02-5391, 2004.

20 Cook, B. D., Davis, K. J., Wang, W., Desai, A., Berger, B. W., Teclaw, R. M., Martin, J. G.,  
21 Bolstad, P. V., Bakwin, P. S., Yi, C., and Heilman, W.: Carbon exchange and venting  
22 anomalies in an upland deciduous forest in northern Wisconsin, USA, *Agric. For. Meteorol.*,  
23 126, 271-295, 10.1016/j.agrformet.2004.06.008, 2004.



1 Cook, B. D., Bolstad, P. V., Martin, J. G., Heinsch, F. A., Davis, K. J., Wang, W., Desai, A. R.,  
2 and Teclaw, R. M.: Using light-use and production efficiency models to predict  
3 photosynthesis and net carbon exchange during forest canopy disturbance, *Ecosystems*, 11,  
4 26-44, 10.1007/s10021-007-9105-0, 2008.

5 Coursolle, C., Margolis, H. A., Giasson, M. A., Bernier, P. Y., Amiro, B. D., Arain, M. A., Barr,  
6 A. G., Black, T. A., Goulden, M. L., McCaughey, J. H., Chen, J. M., Dunn, A. L., Grant, R.  
7 F., and Lafleur, P. M.: Influence of stand age on the magnitude and seasonality of carbon  
8 fluxes in Canadian forests, *Agric. For. Meteorol.*, 165, 136-148,  
9 10.1016/j.agrformet.2012.06.011, 2012.

10 Curtis, P. S., Hanson, P. J., Bolstad, P., Barford, C., Randolph, J. C., Schmid, H. P., and Wilson,  
11 K. B.: Biometric and eddy-covariance based estimates of annual carbon storage in five eastern  
12 North American deciduous forests, *Agric. For. Meteorol.*, 113, 3-19, 10.1016/S0168-  
13 1923(02)00099-0, 2002.

14 Dangal, S. R. S., Felzer, B. S., and Hurteau, M. D.: Effects of agriculture and timber harvest on  
15 carbon sequestration in the eastern US forests, *Journal of Geophysical Research:*  
16 *Biogeosciences*, 119, 36-54, 10.1002/2013JG002409, 2014.

17 DeLucia, E. H., Drake, J. E., Thomas, R. B., and Gonzalez-Meler, M.: Forest carbon use  
18 efficiency: Is respiration a constant fraction of gross primary production?, *Glob. Change*  
19 *Biol.*, 13, 1157-1167, 2007.

20 Desai, A. R., Bolstad, P. V., Cook, B. D., Davis, K. J., and Carey, E. V.: Comparing net  
21 ecosystem exchange of carbon dioxide between an old-growth and mature forest in the upper  
22 Midwest, USA, *Agric. For. Meteorol.*, 128, 33-55,  
23 <http://dx.doi.org/10.1016/j.agrformet.2004.09.005>, 2005.

1 Desai, A. R., Moorcroft, P. R., Bolstad, P. V., and Davis, K. J.: Regional carbon fluxes from an  
2 observationally constrained dynamic ecosystem model: Impacts of disturbance, CO<sub>2</sub>  
3 fertilization, and heterogeneous land cover, *Journal of Geophysical Research: Biogeosciences*,  
4 112, G01017, 10.1029/2006JG000264, 2007.

5 Desai, A. R., Noormets, A., Bolstad, P. V., Chen, J., Cook, B. D., Davis, K. J., Euskirchen, E. S.,  
6 Gough, C., Martin, J. G., Ricciuto, D. M., Schmid, H. P., Tang, J., and Wang, W.: Influence  
7 of vegetation and seasonal forcing on carbon dioxide fluxes across the Upper Midwest, USA:  
8 Implications for regional scaling, *Agric. For. Meteorol.*, 148, 288-308,  
9 <http://dx.doi.org/10.1016/j.agrformet.2007.08.001>, 2008.

10 Etheridge, D. M., Steele, L. P., Langenfelds, R. L., Francey, R. J., Barnola, J. M., and Morgan,  
11 V. I.: Natural and anthropogenic changes in atmospheric CO<sub>2</sub> over the last 1000 years from  
12 air in Antarctic ice and firn, *Journal of Geophysical Research: Atmospheres*, 101, 4115-4128,  
13 10.1029/95JD03410, 1996.

14 Euskirchen, E. S., Chen, J., Gustafson, E. J., and Ma, S.: Soil respiration at dominant patch types  
15 within a managed northern Wisconsin landscape, *Ecosystems*, 6, 595-607,  
16 10.1007/PL00021505, 2003.

17 Galloway, J. N., Dentener, F. J., Capone, D. G., Boyer, E. W., Howarth, R. W., Seitzinger, S. P.,  
18 Asner, G. P., Cleveland, C. C., Green, P. A., Holland, E. A., Karl, D. M., Michaels, A. F.,  
19 Porter, J. H., Townsend, A. R., and Vöosmarty, C. J.: Nitrogen cycles: past, present, and  
20 future, *Biogeochemistry*, 70, 153-226, 10.1007/s10533-004-0370-0, 2004.

21 Gough, C. M., Vogel, C. S., Harrold, K. H., George, K., and Curtis, P. S.: The legacy of harvest  
22 and fire on ecosystem carbon storage in a north temperate forest, *Glob. Change Biol.*, 13,  
23 1935-1949, 10.1111/j.1365-2486.2007.01406.x, 2007.

1 Gough, C. M., Vogel, C. S., Schmid, H. P., Su, H. B., and Curtis, P. S.: Multi-year convergence  
2 of biometric and meteorological estimates of forest carbon storage, *Agric. For. Meteorol.*,  
3 148, 158-170, 2008.

4 Goulden, M. L., McMillan, A. M. S., Winston, G. C., Rocha, A. V., Manies, K. L., Harden, J.  
5 W., and Bond-Lamberty, B. P.: Patterns of NPP, GPP, respiration, and NEP during boreal  
6 forest succession, *Glob. Change Biol.*, 17, 855-871, 10.1111/j.1365-2486.2010.02274.x, 2011.

7 Grant, R. F., Barr, A. G., Black, T. A., Margolis, H. A., Dunn, A. L., Metsaranta, J., Wang, S.,  
8 McCaughey, J. H., and Bourque, C. A.: Interannual variation in net ecosystem productivity of  
9 Canadian forests as affected by regional weather patterns - A Fluxnet-Canada synthesis,  
10 *Agric. For. Meteorol.*, 149, 2022-2039, 2009.

11 Humphreys, E. R., Black, T. A., Morgenstern, K., Cai, T., Drewitt, G. B., Nesic, Z., and  
12 Trofymow, J. A.: Carbon dioxide fluxes in coastal Douglas-fir stands at different stages of  
13 development after clearcut harvesting, *Agric. For. Meteorol.*, 140, 6-22, 2006.

14 Johnson, D. W., and Curtis, P. S.: Effects of forest management on soil C and N storage: meta  
15 analysis, *For. Ecol. Manage.*, 140, 227-238, 10.1016/S0378-1127(00)00282-6, 2001.

16 Kranabetter, J. M., Sanborn, P., Chapman, B. K., and Dube, S.: The Contrasting Response to Soil  
17 Disturbance between Lodgepole Pine and Hybrid White Spruce in Subboreal Forests, *Soil  
18 Sci. Soc. Am. J.*, 70, 1591-1599, 10.2136/sssaj2006.0081, 2006.

19 Kurz, W. A., Dymond, C. C., Stinson, G., Rampley, G. J., Neilson, E. T., Carroll, A. L., Ebata,  
20 T., and Safranyik, L.: Mountain pine beetle and forest carbon feedback to climate change,  
21 *Nature*, 452, 987-990, 2008.

22 Landsberg, J.: Modelling forest ecosystems: state of the art, challenges, and future directions,  
23 *Can. J. For. Res.*, 33, 385-397, 10.1139/x02-129, 2003.

1 Law, B. E., Sun, O. J., Campbell, J., Van Tuyl, S., and Thornton, P. E.: Changes in carbon  
2 storage and fluxes in a chronosequence of ponderosa pine, *Glob. Change Biol.*, 9, 510-524,  
3 10.1046/j.1365-2486.2003.00624.x, 2003.

4 Ma, Z., Peng, C., Zhu, Q., Chen, H., Yu, G., Li, W., Zhou, X., Wang, W., and Zhang, W.:  
5 Regional drought-induced reduction in the biomass carbon sink of Canada's boreal forests,  
6 *Proc. Natl. Acad. Sci. U. S. A.*, 109, 2423-2427, 10.1073/pnas.1111576109, 2012.

7 Magnani, F., Mencuccini, M., Borghetti, M., Berbigier, P., Berninger, F., Delzon, S., Grelle, A.,  
8 Hari, P., Jarvis, P. G., Kolari, P., Kowalski, A. S., Lankreijer, H., Law, B. E., Lindroth, A.,  
9 Loustau, D., Manca, G., Moncrieff, J. B., Rayment, M., Tedeschi, V., Valentini, R., and  
10 Grace, J.: The human footprint in the carbon cycle of temperate and boreal forests, *Nature*,  
11 447, 849-851, 2007.

12 Martin, J., and Bolstad, P.: Annual soil respiration in broadleaf forests of northern Wisconsin:  
13 influence of moisture and site biological, chemical, and physical characteristics,  
14 *Biogeochemistry*, 73, 149-182, 10.1007/s10533-004-5166-8, 2005.

15 Masek, J. G., Cohen, W. B., Leckie, D., Wulder, M. A., Vargas, R., de Jong, B., Healey, S., Law,  
16 B., Birdsey, R., Houghton, R. A., Mildrexler, D., Goward, S., and Smith, W. B.: Recent rates  
17 of forest harvest and conversion in North America, *J. Geophys. Res.*, 116, G00K03,  
18 10.1029/2010jg001471, 2011.

19 McDowell, N. G.: Mechanisms linking drought, hydraulics, carbon metabolism, and vegetation  
20 mortality, *Plant Physiol.*, 155, 1051-1059, 2011.

21 McDowell, N. G., Fisher, R. A., Xu, C., Domec, J. C., Hölttä, T., Mackay, D. S., Sperry, J. S.,  
22 Boutz, A., Dickman, L., Gehres, N., Limousin, J. M., Macalady, A., Martínez-Vilalta, J.,  
23 Mencuccini, M., Plaut, J. A., Ogée, J., Pangle, R. E., Rasse, D. P., Ryan, M. G., Sevanto, S.,

1 Waring, R. H., Williams, A. P., Yopez, E. A., and Pockman, W. T.: Evaluating theories of  
2 drought-induced vegetation mortality using a multimodel–experiment framework, *New*  
3 *Phytol.*, 200, 304-321, 10.1111/nph.12465, 2013.

4 McGuire, A. D., Sitch, S., Clein, J. S., Dargaville, R., Esser, G., Foley, J., Heimann, M., Joos, F.,  
5 Kaplan, J., Kicklighter, D. W., Meier, R. A., Melillo, J. M., Moore, B., Prentice, I. C.,  
6 Ramankutty, N., Reichenau, T., Schloss, A., Tian, H., Williams, L. J., and Wittenberg, U.:  
7 Carbon balance of the terrestrial biosphere in the Twentieth Century: Analyses of CO<sub>2</sub>,  
8 climate and land use effects with four process-based ecosystem models, *Glob. Biogeochem.*  
9 *Cycle*, 15, 183-206, 10.1029/2000GB001298, 2001.

10 Medvigy, D., Wofsy, S. C., Munger, J. W., Hollinger, D. Y., and Moorcroft, P. R.: Mechanistic  
11 scaling of ecosystem function and dynamics in space and time: Ecosystem Demography  
12 model version 2, *J. Geophys. Res.*, 114, G01002, 10.1029/2008jg000812, 2009.

13 Miller, D. A., and White, R. A.: A Conterminous United States Multilayer Soil Characteristics  
14 Dataset for Regional Climate and Hydrology Modeling, *Earth Interactions*, 2, 1-26,  
15 10.1175/1087-3562(1998)002<0001:ACUSMS>2.3.CO;2, 1998.

16 Misson, L., Baldocchi, D. D., Black, T. A., Blanken, P. D., Brunet, Y., Curiel Yuste, J., Dorsey,  
17 J. R., Falk, M., Granier, A., Irvine, M. R., Jarosz, N., Lamaud, E., Launiainen, S., Law, B. E.,  
18 Longdoz, B., Loustau, D., McKay, M., Paw U, K. T., Vesala, T., Vickers, D., Wilson, K. B.,  
19 and Goldstein, A. H.: Partitioning forest carbon fluxes with overstory and understory eddy-  
20 covariance measurements: A synthesis based on FLUXNET data, *Agric. For. Meteorol.*, 144,  
21 14-31, 2007.

22 Mkhabela, M. S., Amiro, B. D., Barr, A. G., Black, T. A., Hawthorne, I., Kidston, J.,  
23 McCaughey, J. H., Orchansky, A. L., Nesic, Z., Sass, A., Shashkov, A., and Zha, T.:

1 Comparison of carbon dynamics and water use efficiency following fire and harvesting in  
2 Canadian boreal forests, *Agric. For. Meteorol.*, 149, 783-794,  
3 <http://dx.doi.org/10.1016/j.agrformet.2008.10.025>, 2009.

4 Noormets, A., Chen, J., and Crow, T.: Age-dependent changes in ecosystem carbon fluxes in  
5 managed forests in Northern Wisconsin, USA, *Ecosystems*, 10, 187-203, 2007.

6 Noormets, A., Desai, A. R., Cook, B. D., Euskirchen, E. S., Ricciuto, D. M., Davis, K. J.,  
7 Bolstad, P. V., Schmid, H. P., Vogel, C. V., Carey, E. V., Su, H. B., and Chen, J.: Moisture  
8 sensitivity of ecosystem respiration: Comparison of 14 forest ecosystems in the Upper Great  
9 Lakes Region, USA, *Agric. For. Meteorol.*, 148, 216-230, 2008.

10 Odum, E. P.: The Strategy of Ecosystem Development, *Science*, 164, 262-270,  
11 [10.1126/science.164.3877.262](https://doi.org/10.1126/science.164.3877.262), 1969.

12 Ollinger, S. V., Aber, J. D., Reich, P. B., and Freuder, R. J.: Interactive effects of nitrogen  
13 deposition, tropospheric ozone, elevated CO<sub>2</sub> and land use history on the carbon dynamics of  
14 northern hardwood forests, *Glob. Change Biol.*, 8, 545-562, [10.1046/j.1365-](https://doi.org/10.1046/j.1365-2486.2002.00482.x)  
15 [2486.2002.00482.x](https://doi.org/10.1046/j.1365-2486.2002.00482.x), 2002.

16 Pan, Y., Birdsey, R., Hom, J., and McCullough, K.: Separating effects of changes in atmospheric  
17 composition, climate and land-use on carbon sequestration of U.S. Mid-Atlantic temperate  
18 forests, *For. Ecol. Manage.*, 259, 151-164, 2009.

19 Pan, Y., Birdsey, R. A., Fang, J., Houghton, R., Kauppi, P. E., Kurz, W. A., Phillips, O. L.,  
20 Shvidenko, A., Lewis, S. L., Canadell, J. G., Ciais, P., Jackson, R. B., Pacala, S. W.,  
21 McGuire, A. D., Piao, S., Rautiainen, A., Sitch, S., and Hayes, D.: A Large and Persistent  
22 Carbon Sink in the World's Forests, *Science*, 333, 988-993, [10.1126/science.1201609](https://doi.org/10.1126/science.1201609), 2011.

1 Peckham, S. D., Gower, S. T., and Buongiorno, J.: Estimating the carbon budget and maximizing  
2 future carbon uptake for a temperate forest region in the U.S, *Carbon Balance and*  
3 *Management*, 7, doi:10.1186/1750-0680-7-6, 2012.

4 Peichl, M., and Arain, M. A.: Above- and belowground ecosystem biomass and carbon pools in  
5 an age-sequence of temperate pine plantation forests, *Agric. For. Meteorol.*, 140, 51-63, 2006.

6 Peng, C., Ma, Z., Lei, X., Zhu, Q., Chen, H., Wang, W., Liu, S., Li, W., Fang, X., and Zhou, X.:  
7 A drought-induced pervasive increase in tree mortality across Canada's boreal forests, *Nature*  
8 *Clim. Change*, 1, 467-471, 10.1038/nclimate1293, 2011.

9 Peters, E. B., Wythers, K. R., Bradford, J. B., and Reich, P. B.: Influence of disturbance on  
10 temperate forest productivity, *Ecosystems*, 16, 95-110, 10.1007/s10021-012-9599-y, 2013.

11 Powell, T. L., Galbraith, D. R., Christoffersen, B. O., Harper, A., Imbuzeiro, H. M. A., Rowland,  
12 L., Almeida, S., Brando, P. M., da Costa, A. C. L., Costa, M. H., Levine, N. M., Malhi, Y.,  
13 Saleska, S. R., Sotta, E., Williams, M., Meir, P., and Moorcroft, P. R.: Confronting model  
14 predictions of carbon fluxes with measurements of Amazon forests subjected to experimental  
15 drought, *New Phytol.*, 200, 350-365, 10.1111/nph.12390, 2013.

16 Powers, M. D., Kolka, R. K., Bradford, J. B., Palik, B. J., Fraver, S., and Jurgensen, M. F.:  
17 Carbon stocks across a chronosequence of thinned and unmanaged red pine (*Pinus resinosa*)  
18 stands, *Ecol. Appl.*, 22, 1297-1307, 10.1890/11-0411.1, 2012.

19 Pregitzer, K. S., and Euskirchen, E. S.: Carbon cycling and storage in world forests: biome  
20 patterns related to forest age, *Glob. Change Biol.*, 10, 2052-2077, 2004.

21 Raich, J. W., Rastetter, E. B., Melillo, J. M., Kicklighter, D. W., Steudler, P. A., Peterson, B. J.,  
22 Grace, A. L., Moore, B., and Vorosmarty, C. J.: Potential Net Primary Productivity in South  
23 America: Application of a Global Model, *Ecol. Appl.*, 1, 399-429, 10.2307/1941899, 1991.

1 Ryu, S.-R., Chen, J., Noormets, A., Bresee, M. K., and Ollinger, S. V.: Comparisons between  
2 PnET-Day and eddy covariance based gross ecosystem production in two Northern Wisconsin  
3 forests, *Agric. For. Meteorol.*, 148, 247-256, 10.1016/j.agrformet.2007.08.005, 2008.

4 Schwalm, C. R., Williams, C. A., Schaefer, K., Baldocchi, D., Black, T. A., Goldstein, A. H.,  
5 Law, B. E., Oechel, W. C., Paw U, K. T., and Scott, R. L.: Reduction in carbon uptake during  
6 turn of the century drought in western North America, *Nature Geosci.*, 5, 551-556,  
7 <http://www.nature.com/ngeo/journal/v5/n8/abs/ngeo1529.html#supplementary-information>,  
8 2012.

9 Smith, B., Prentice, I. C., and Sykes, M. T.: Representation of vegetation dynamics in the  
10 modelling of terrestrial ecosystems: Comparing two contrasting approaches within European  
11 climate space, *Glob. Ecol. Biogeogr.*, 10, 621-637, 2001.

12 Sprugel, G. D.: Natural Disturbance and Ecosystem Energetics, in: *The Ecology of Natural*  
13 *Disturbance and Patch Dynamics*, edited by: Pickett, S. T. A., and White, P. S., Academic  
14 Press, Inc, New York, 335-352, 1985.

15 Tang, J., Bolstad, P. V., and Martin, J. G.: Soil carbon fluxes and stocks in a Great Lakes forest  
16 chronosequence, *Glob. Change Biol.*, 15, 145-155, 10.1111/j.1365-2486.2008.01741.x, 2009.

17 Tang, J., Luysaert, S., Richardson, A. D., Kutsch, W., and Janssens, I. A.: Steeper declines in  
18 forest photosynthesis than respiration explain age-driven decreases in forest growth,  
19 *Proceedings of the National Academy of Sciences*, 10.1073/pnas.1320761111, 2014.

20 Thornton, P. E., M. M Thornton, B. W Mayer, N. Wilhelmi, Y. Wei, and R.B. Cook: Daymet:  
21 Daily surface weather on a 1 km grid for North America, 1980 - 2011. , Acquired online  
22 (<http://daymet.ornl.gov/>) on [05/02/2013] from Oak Ridge National Laboratory Distributed



1 Active Archive Center, Oak Ridge, Tennessee, U.S.A.  
2 doi:10.3334/ORNLDAAC/Daymet\_V2., 2012.

3 van Mantgem, P. J., Stephenson, N. L., Byrne, J. C., Daniels, L. D., Franklin, J. F., Fulé, P. Z.,  
4 Harmon, M. E., Larson, A. J., Smith, J. M., Taylor, A. H., and Veblen, T. T.: Widespread  
5 increase of tree mortality rates in the western United States, *Science*, 323, 521, 2009.

6 Wang, W., Peng, C., Kneeshaw, D. D., Larocque, G. R., and Luo, Z.: Drought-induced tree  
7 mortality: ecological consequences, causes, and modeling, *Environ. Rev.*, 20, 109-121,  
8 10.1139/a2012-004, 2012a.

9 Wang, W., Peng, C., Kneeshaw, D. D., Larocque, G. R., Song, X., and Zhou, X.: Quantifying the  
10 effects of climate change and harvesting on carbon dynamics of boreal aspen and jack pine  
11 forests using the TRIPLEX-Management model, *For. Ecol. Manage.*, 281, 152-162,  
12 10.1016/j.foreco.2012.06.028, 2012b.

13 Wang, W., Peng, C., Kneeshaw, D. D., Larocque, G. R., Lei, X., Zhu, Q., Song, X., and Tong,  
14 Q.: Modeling the effects of varied forest management regimes on carbon dynamics in jack  
15 pine stands under climate change, *Can. J. For. Res.*, 43, 469-479, 10.1139/cjfr-2012-0320,  
16 2013.

17 Williams, C. A., Collatz, G. J., Masek, J., and Goward, S. N.: Carbon consequences of forest  
18 disturbance and recovery across the conterminous United States, *Glob. Biogeochem. Cycle*,  
19 26, GB1005, 10.1029/2010gb003947, 2012.

20 Willmott, C. J.: Some comments on the evaluation of model performance, *Bull. Am. Meteor.*  
21 *Soc.*, 63, 1309-1313, doi:10.1175/1520-0477(1982)063<1309:SCOTEO>2.0.CO;2, 1982.

22 Wisconsin Department of Natural Resources: Wisconsin Forest Management Guidelines, PUB-  
23 FR-226. <http://dnr.wi.gov/topic/ForestManagement/guidelines.html>, 2011.

1 Xiao, J., Zhuang, Q., Liang, E., Shao, X., McGuire, A. D., Moody, A., Kicklighter, D. W., and  
2 Melillo, J. M.: Twentieth-century droughts and their impacts on terrestrial carbon cycling in  
3 China, *Earth Interactions*, 13, 1-31, 10.1175/2009EI275.1, 2009.

4 Xiao, J., Davis, K. J., Urban, N. M., Keller, K., and Saliendra, N. Z.: Upscaling carbon fluxes  
5 from towers to the regional scale: Influence of parameter variability and land cover  
6 representation on regional flux estimates, *Journal of Geophysical Research G:  
7 Biogeosciences*, 116, G00J06, 10.1029/2010JG001568, 2011.

8 Xiao, J., Davis, K. J., Urban, N. M., and Keller, K.: Uncertainty in model parameters and  
9 regional carbon fluxes: A model-data fusion approach, *Agric. For. Meteorol.*, 189–190, 175-  
10 186, <http://dx.doi.org/10.1016/j.agrformet.2014.01.022>, 2014.

11 Yanai, R. D., Currie, W. S., and Goodale, C. L.: Soil carbon dynamics after forest harvest: An  
12 ecosystem paradigm reconsidered, *Ecosystems*, 6, 197-212, 10.1007/s10021-002-0206-5,  
13 2003.

14 Zha, T., Barr, A. G., Black, T. A., McCaughey, J. H., Bhatti, J., Hawthorne, I., Krishnan, P.,  
15 Kidston, J., Saigusa, N., Shashkov, A., and Nesic, Z.: Carbon sequestration in boreal jack pine  
16 stands following harvesting, *Glob. Change Biol.*, 15, 1475-1487, 10.1111/j.1365-  
17 2486.2008.01817.x, 2009.

18 Zhao, M., and Running, S. W.: Drought-induced reduction in global terrestrial net primary  
19 production from 2000 through 2009, *Science*, 329, 940-943, 10.1126/science.1192666, 2010.

20

1 **Tables**

2 Table 1 Site characteristics for two chronosequences of deciduous broadleaf forests (DBF) and evergreen needleleaf forests (ENF) in  
 3 Upper Midwest region of Wisconsin and Michigan, United States.

Site	ID	Location	Plant function type	Dominant species	Year of recent disturbance	AGC (Mg ha <sup>-1</sup> , 2005)	LAI (m <sup>2</sup> m <sup>-2</sup> , 2002)	Data period	Reference
Clearcut young hardwood	YHW	46.72°N 91.25°W	DBF	Aspen, red maple	1999	3.3 (1.3)	0.79 (0.6)	2002	Noormets et al. 2007
Intermediate hardwood	IHW	46.73°N 91.23°W	DBF	Aspen	1984	47.6 (15.6)	3.0	2003	Noormets et al. 2008
Willow creek	WIC	45.80°N 90.08°W	DBF	Sugar maple, basswood, green ash	1875 <sup>a</sup> , 1933	74.9 <sup>b</sup>	5.36 (0.47) <sup>c</sup>	2000-2006	Cook et al., 2008, Curtis et al. 2002
University of Michigan Biological Station	UMBS	45.56°N 84.71°W	DBF	Aspen, white pine, red oak, sugar maple	1920	73.2 (3.1) <sup>d</sup>	3.54 (0.31) <sup>e</sup>	2000-2003	Gough et al. 2008
Young red pine	YRP	46.72°N 91.18°W	ENF	Red pine, jack pine	1993	7.7 (8.3)	0.52 (0.3)	2002	Noormets et al. 2007
Young jack pine	YJP	46.62°N 91.08°W	ENF	Jack pine	1987	4.9 (5.0)	0.93	2004-2005	Noormets et al. 2008
Intermediate red pine	IRP	46.69°N 91.15°W	ENF	Red pine	1980	47.7 (37.3)	3.0	2003	Desai et al. 2008
Mature red pine	MRP	46.74°N 91.17°W	ENF	Red pine, aspen	1939	56.9 (33.1)	2.7 (0.8)	2002-2005	Noormets et al. 2007

4 <sup>a</sup> estimated year of disturbance based on Ameriflux site description in AmeriFlux.  
 5 <sup>b</sup> sum of wood and foliage biomass carbon from Curtis et al., 2002.  
 6 <sup>c</sup> estimated values based on measurements in 1998 to 2000 and 2002 from Cook et al., 2008.,  
 7 <sup>d</sup> value in 2003 from Gough et al. 2008.  
 8 <sup>e</sup> calculated based on multi-year (1999-2003) estimations with litter traps from Gough et al. 2008.

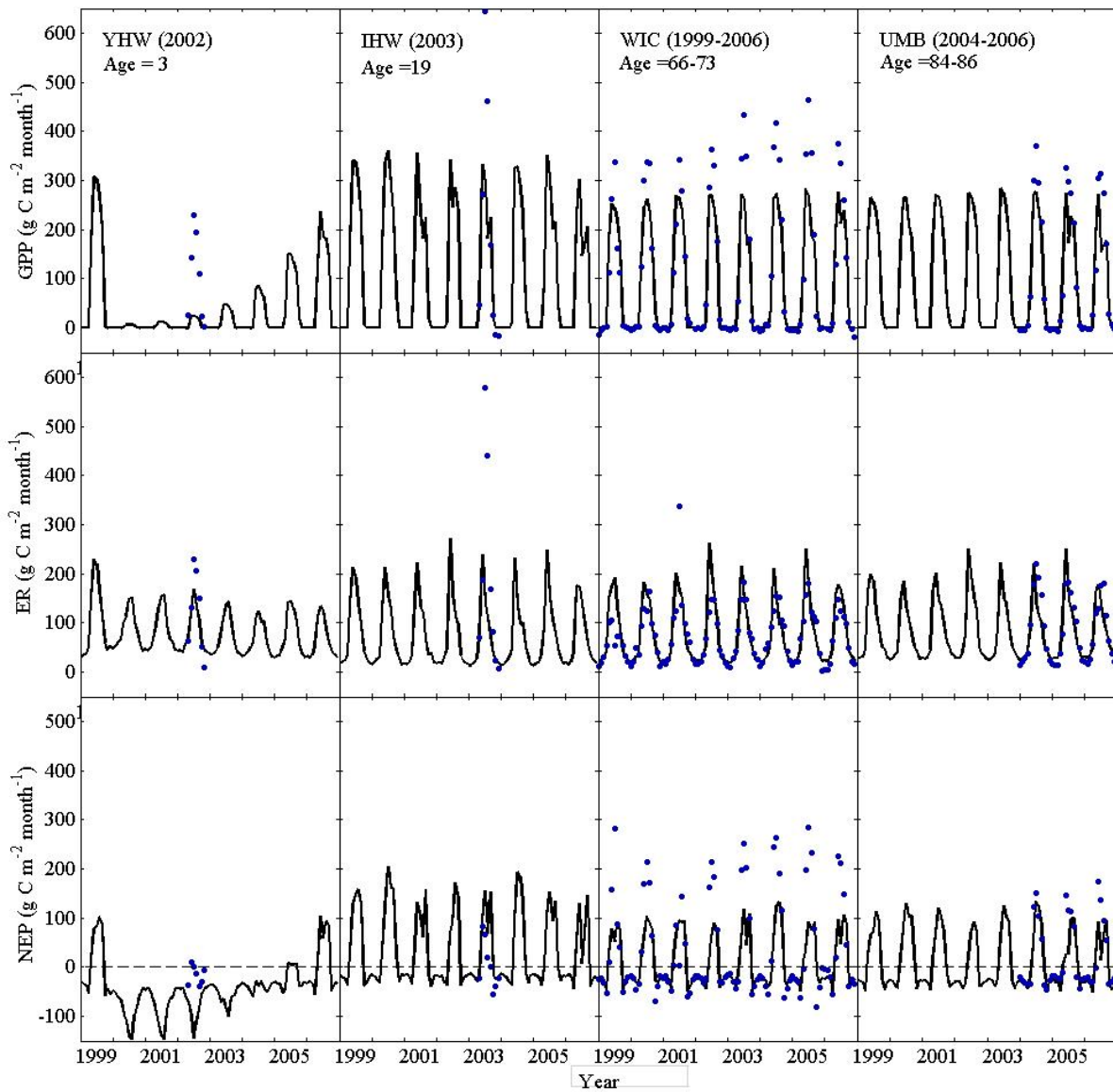
1 Table 2 PnET model performance in monthly carbon fluxes (GPP: gross primary productivity;  
 2 ER: ecosystem respiration; NEP: net ecosystem productivity), leaf area index (LAI), and  
 3 aboveground carbon stock (AGC) for the two chronosequences.

	<b>NRMSE%<sup>a</sup></b>	<b><i>d</i><sup>b</sup></b>	<b>n</b>
<b><i>DBF</i></b>			
GPP	10	0.95	147
ER	10	0.92	147
NEP	17	0.81	147
LAI	33	0.97	4
AGC	42	0.95	4
<b><i>ENF</i></b>			
GPP	28	0.91	64
ER	37	0.88	64
NEP	46	0.58	64
LAI	29	0.96	4
AGC	37	0.94	4
<b><i>Overall</i></b>			
GPP	11	0.94	211
ER	10	0.91	211
NEP	21	0.73	211
LAI	31	0.96	8
AGC	28	0.95	8
Total performance <sup>c</sup>	20	0.90	

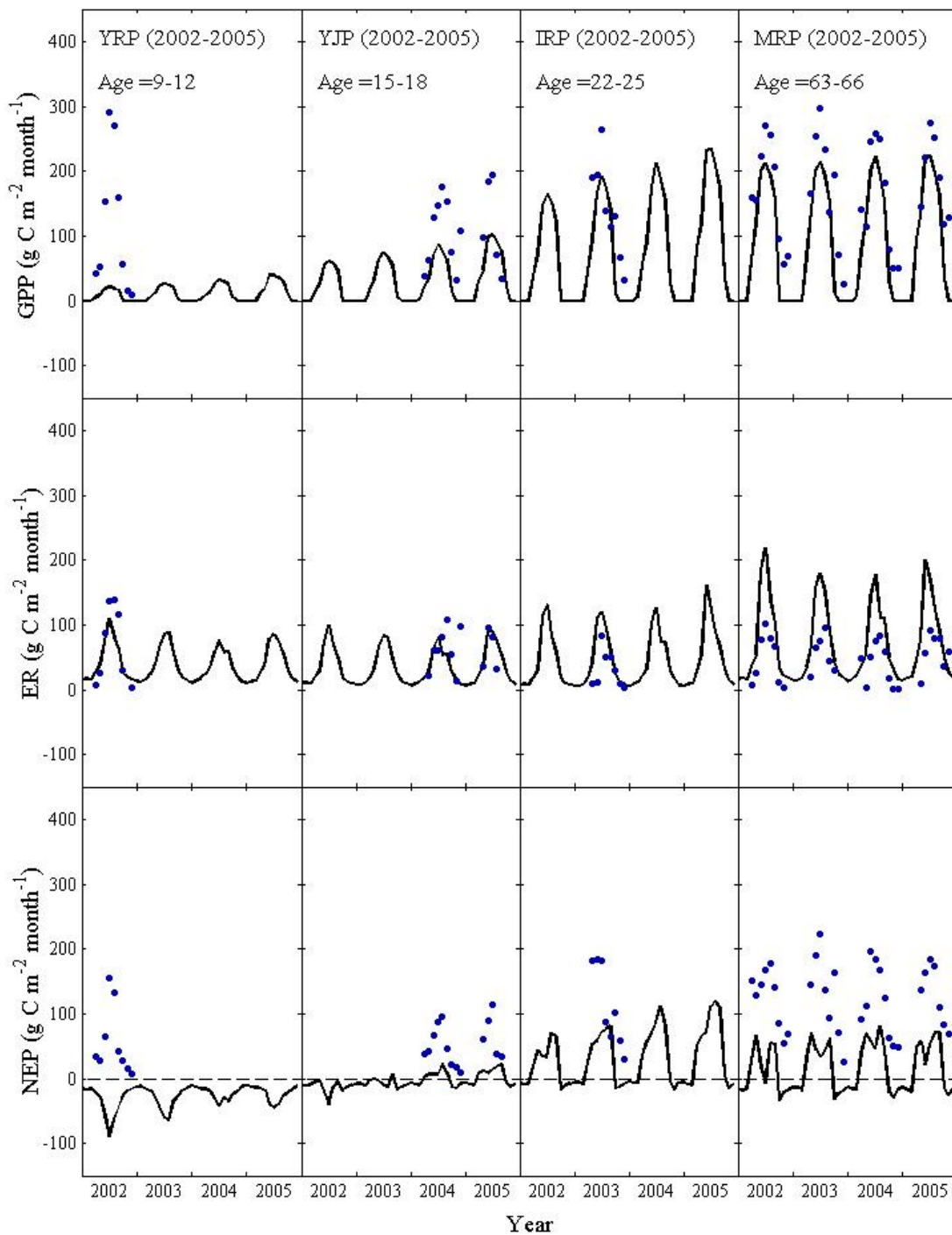
4 <sup>a</sup>Normalized root mean square error.

5 <sup>b</sup>Willmott index.

6 <sup>c</sup>Mean value of evaluating statistics for all tested variables.

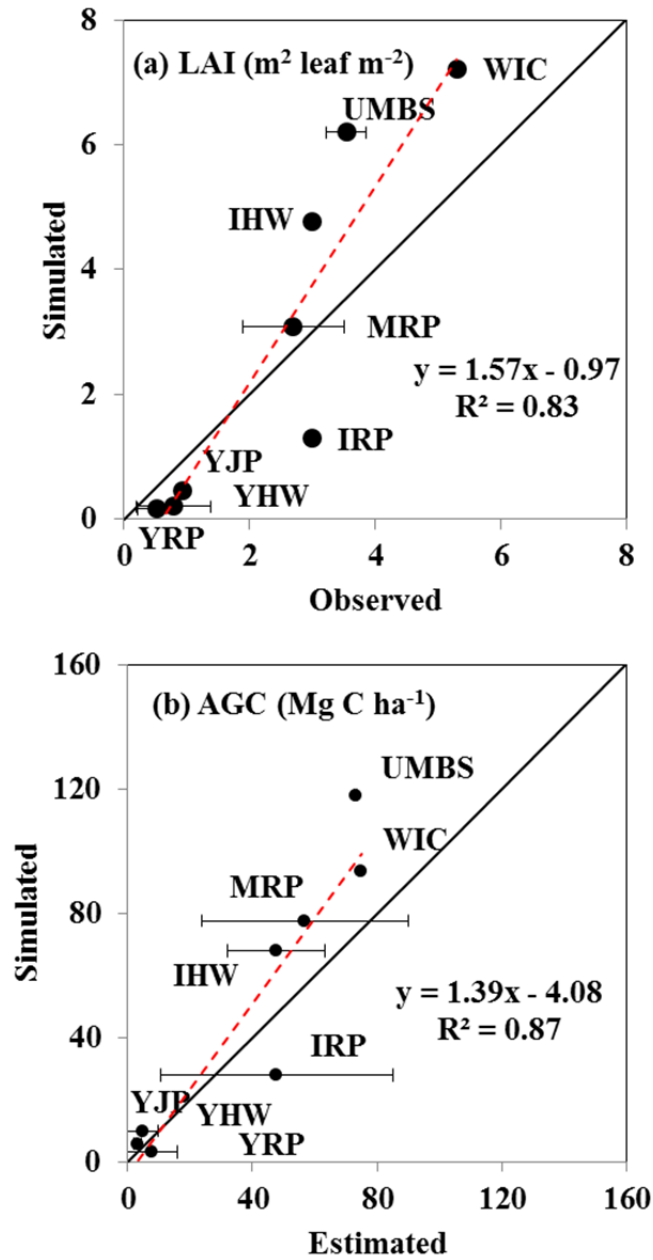


1  
 2 Figure 1. Simulated (lines) and observed (symbols) monthly carbon fluxes: GPP, ER, and NEP  
 3 for the deciduous broadleaf chronosequence sites from 1999-2007.  
 4

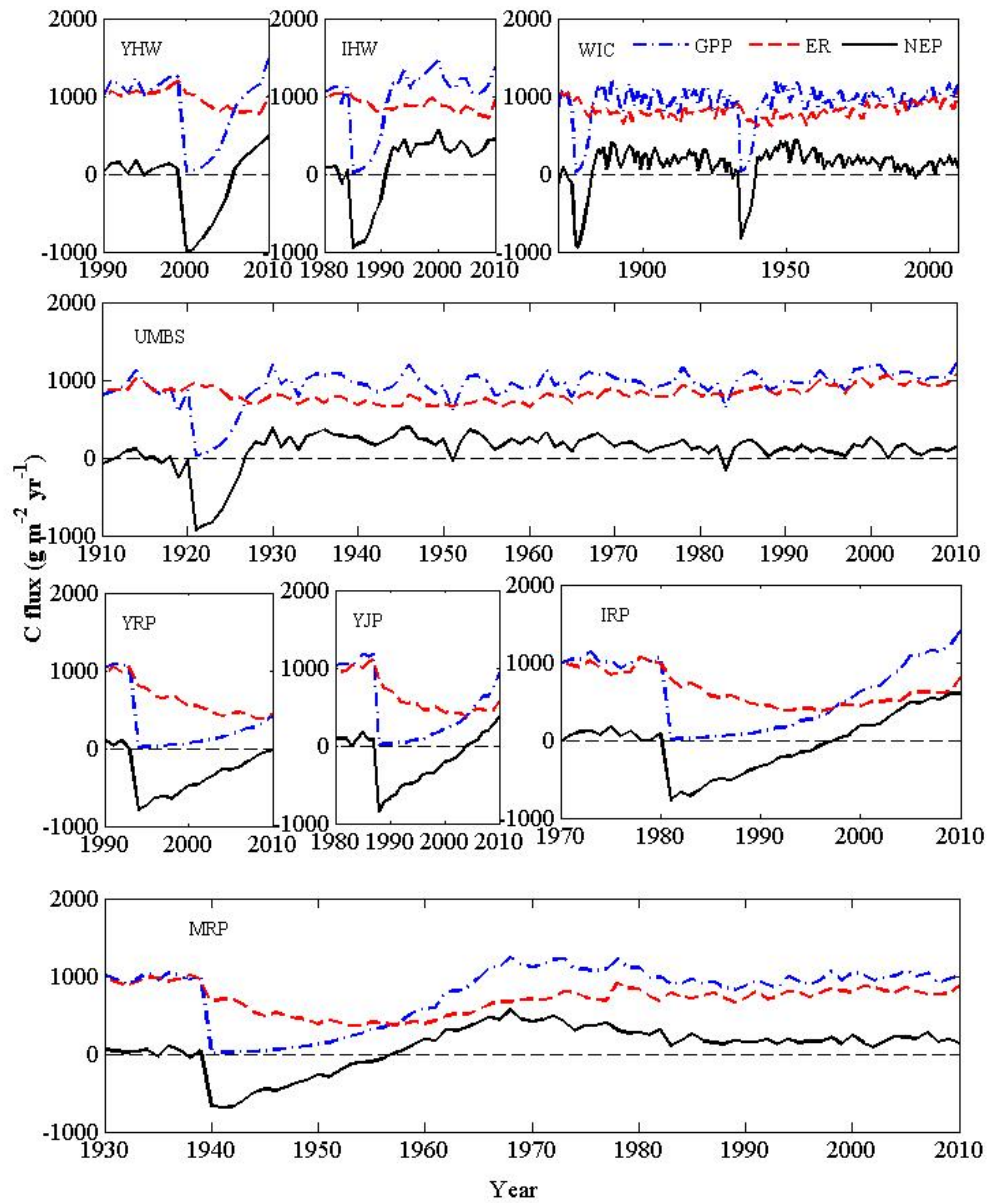


1  
 2 Figure 2. Simulated (lines) and observed (symbols) monthly carbon fluxes: GPP, ER, and NEP  
 3 for the evergreen coniferous chronosequence study sites from 2002-2005.

4



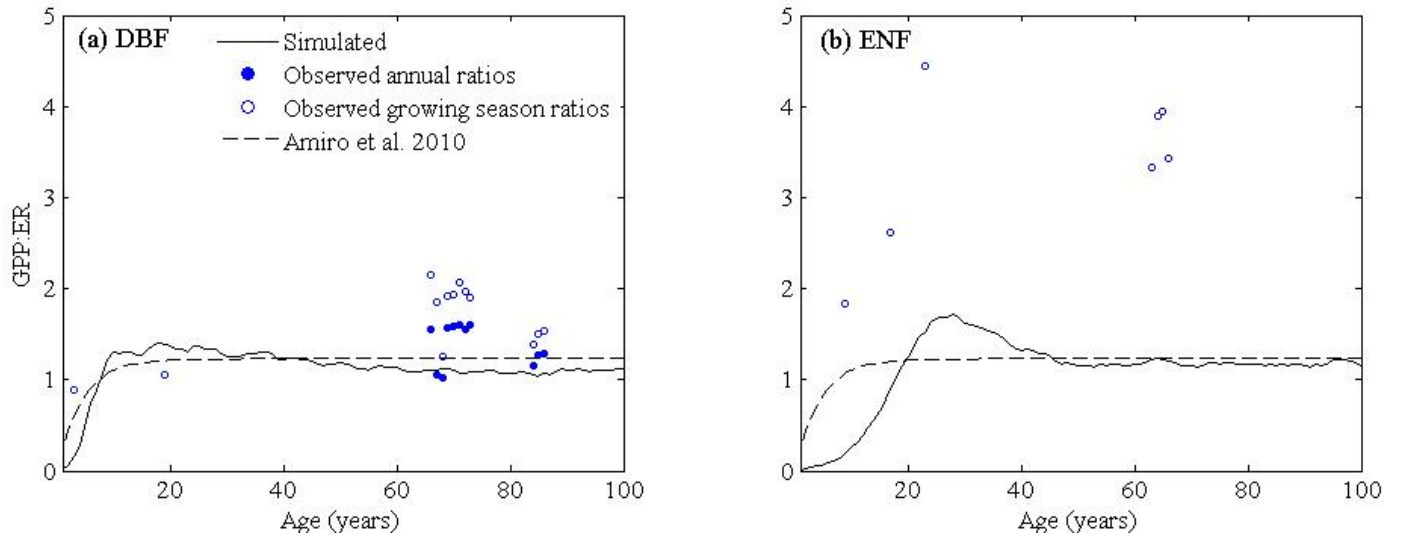
1  
 2 Figure 3. Comparisons of simulated and observed (a) leaf area index (LAI) and (b) aboveground  
 3 carbon stock (AGC) for all eight sites.  
 4



1  
 2 Figure 4. Simulated trajectories of GPP, ER, and NEP for each site based on the site disturbance  
 3 history (Table 1). The time series started from the earliest major disturbance for each site.  
 4



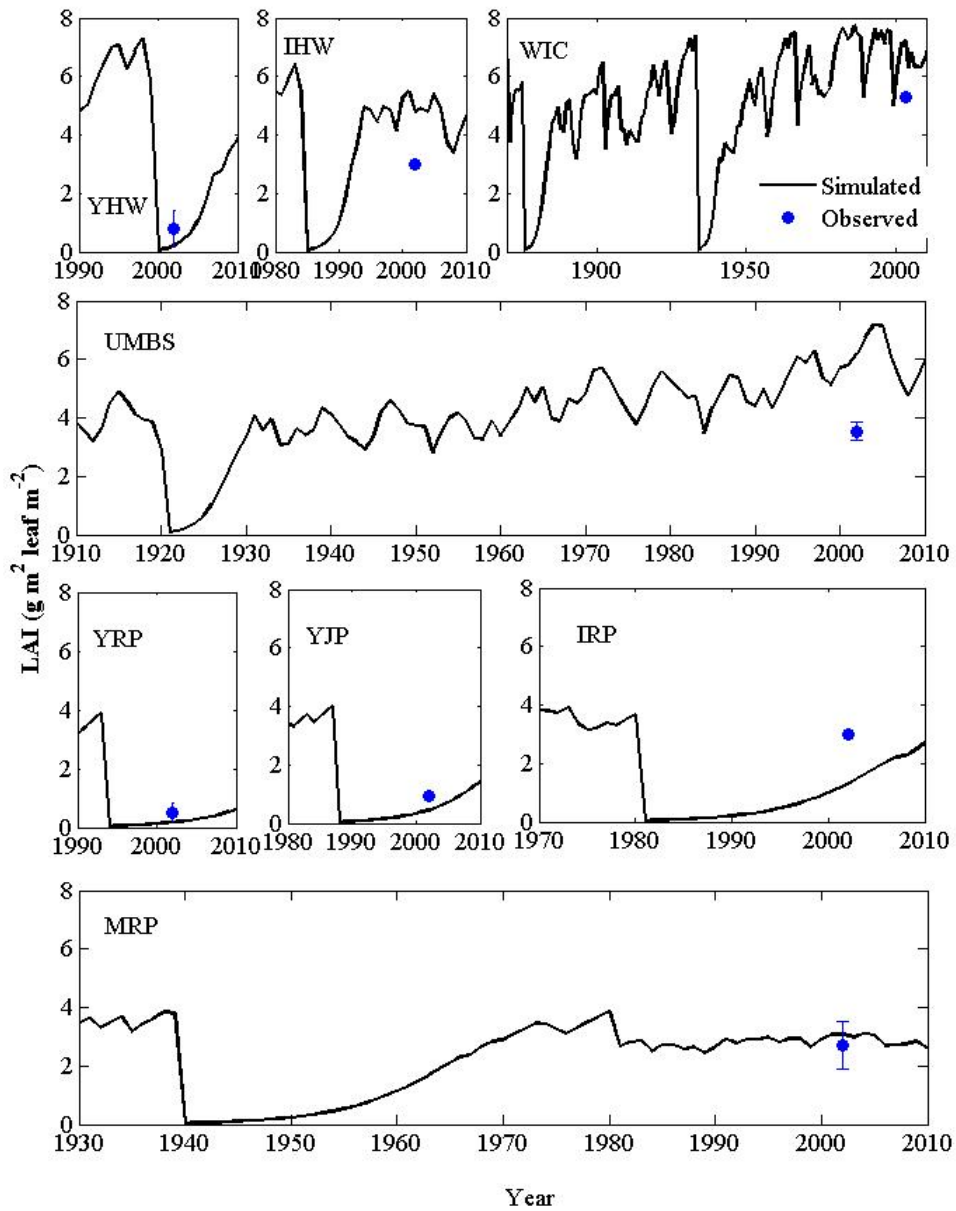
1



2

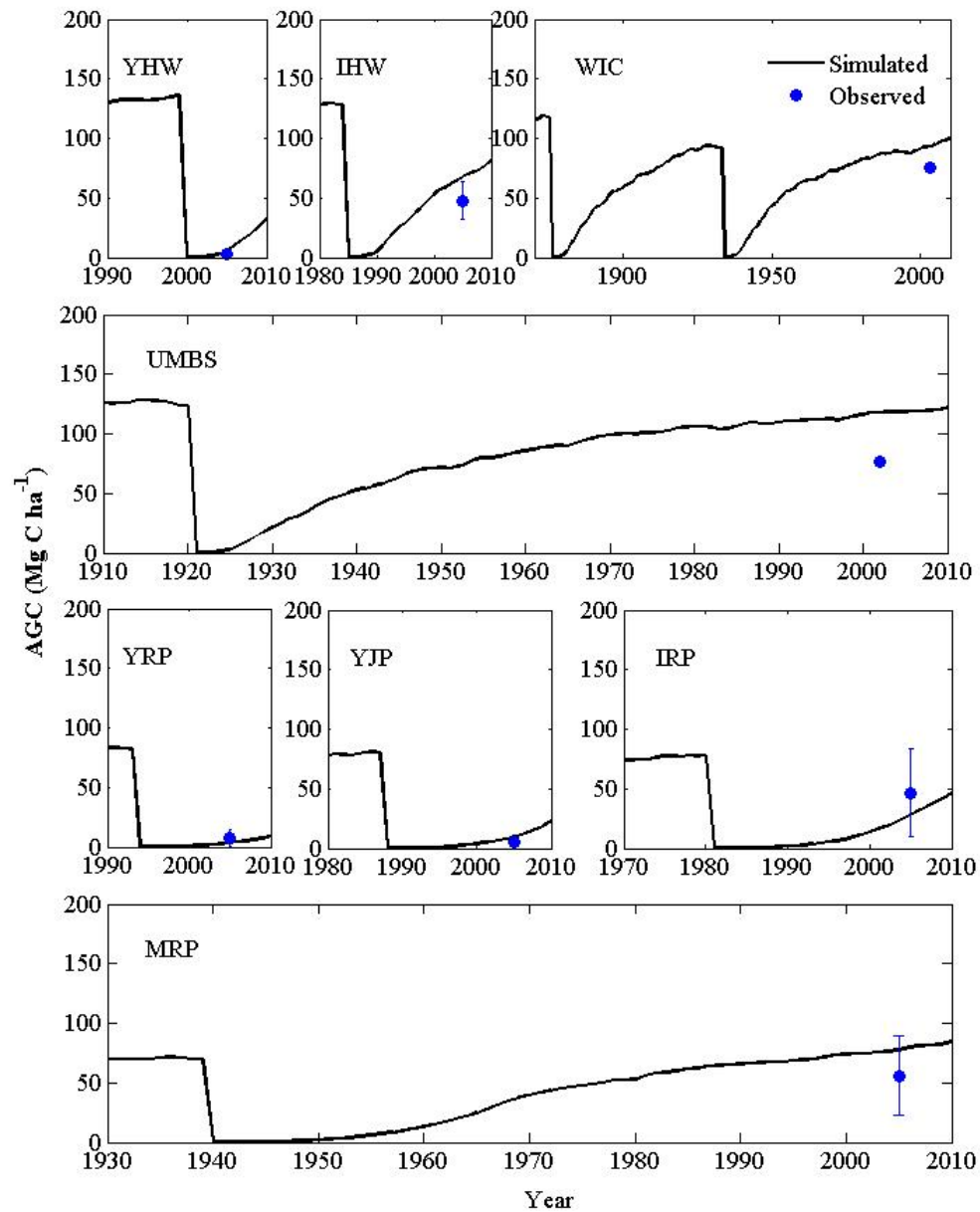
3 Figure 5. Simulated trajectories of the annual GPP/ER ratio with stand age for (a) deciduous  
4 broadleaf forests (DBF) and (b) evergreen coniferous forests (ENF). The dashed line is a fitted  
5 curve derived by Amiro et al. (2010) using eddy covariance observations from chronosequence  
6 forests in North America. Solid and hollow circles represent measured annual and growing  
7 season (May to October) ratios, respectively. The simulated curves were smoothed using a  
8 moving average filter with a span of 5.

9

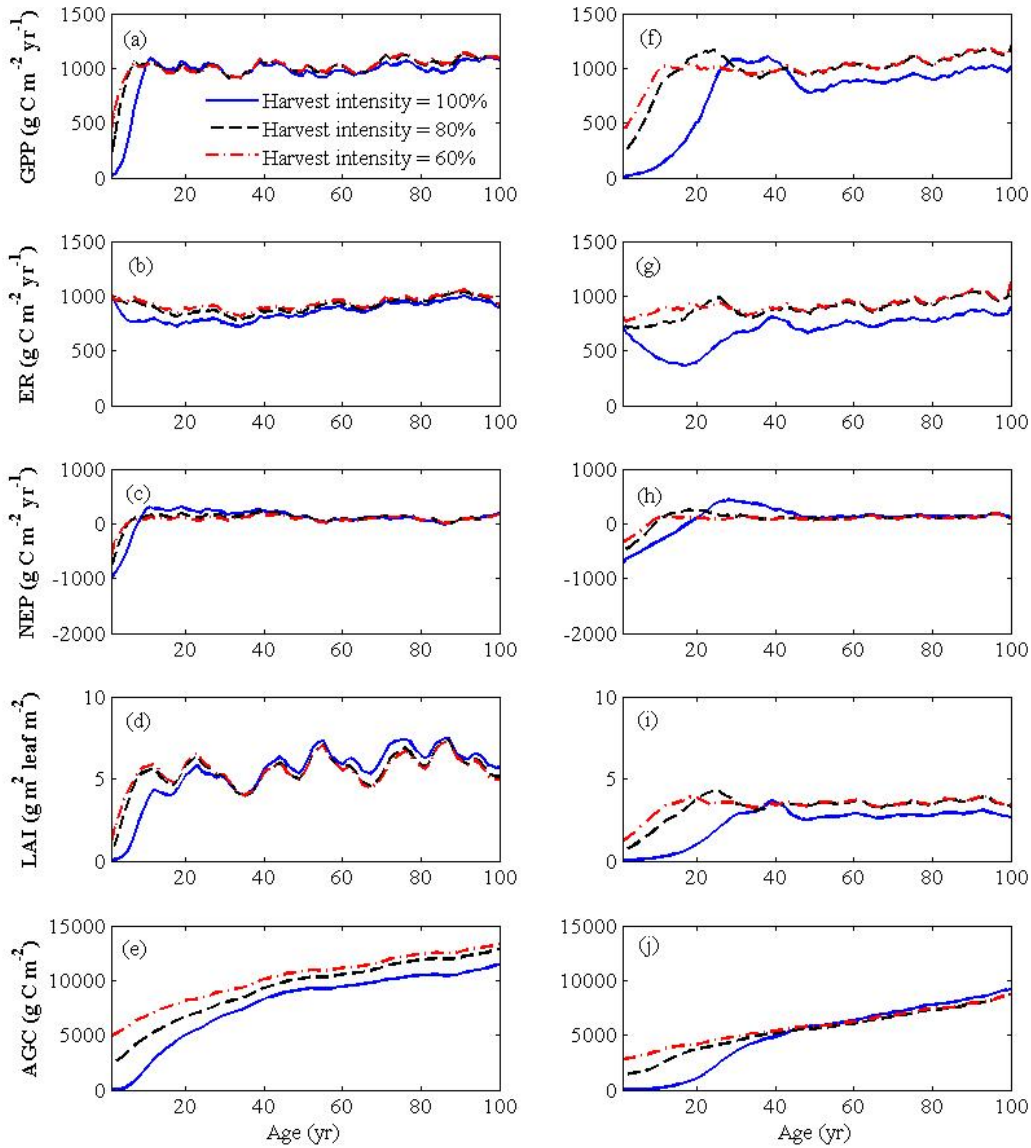


1  
 2 Figure 6. Simulated trajectories of LAI for each site based on the site disturbance history (Table  
 3 1). The time series started from the earliest major disturbance for each site. Symbols represent  
 4 measured LAI.

5



1  
 2 Figure 7. Simulated trajectories of aboveground biomass carbon (AGC) for each site based on  
 3 the site disturbance history (Table 1). The time series started from the earliest major disturbance  
 4 for each site. Symbols represent estimated AGC.



1  
 2 Figure 8. Sensitivity of carbon fluxes (GPP, gross primary production; ER, ecosystem  
 3 respiration; NEP, net ecosystem production) and stand characteristics (LAI: leaf area index;  
 4 AGC: aboveground carbon stock) to changes in harvest intensity (reduced by 0.2 and 0.4  
 5 compared to 1 for assumed clearcuts used in the model tests) for (a-e) deciduous broadleaf  
 6 forests (DBF) at Willow creek and (f-j) evergreen coniferous forests (ENF) at Mature red pine  
 7 site over a 100-yr harvest cycle. The simulated curves were smoothed using a moving average  
 8 filter with a span of 5.

9